Flood inundation modelling using an RProFIM approach based on the scenarios of landuse/landcover change and return periods differences in the upstream Citarum watershed, West Java, Indonesia

Fajar Yulianto (fajar.yulianto@brin.go.id)
National Research and Innovation Agency (BRIN) https://orcid.org/0000-0002-3084-6694

Muhammad Rokhis Khomarudin
National Research and Innovation Agency (BRIN)

Eddy Hermawan
National Research and Innovation Agency (BRIN)

Syarif Budhiman
National Research and Innovation Agency (BRIN)

Parwati Sofan
National Research and Innovation Agency (BRIN)

Galdita Aruba Chulafak
National Research and Innovation Agency (BRIN)

Nunung Puji Nugroho
National Research and Innovation Agency (BRIN)

Randy Prima Brahmantara
National Research and Innovation Agency (BRIN)

Gatot Nugroho
National Research and Innovation Agency (BRIN)

Eko Priyanto
Ministry of Environment and Forestry of the Republic of Indonesia: Kementerian Lingkungan Hidup dan Kehutanan Republik Indonesia

Hana Listi Fitriana
National Research and Innovation Agency (BRIN)

Andie Setiyoko
National Research and Innovation Agency (BRIN)

Anjar Dimara Sakti
ITB: Institut Teknologi Bandung

Research Article

Keywords: Flood inundation, modelling, remote sensing, RProFIM, landuse/landcover change, Citarum, West Java, Indonesia

Posted Date: June 22nd, 2022

DOI: https://doi.org/10.21203/rs.3.rs-1724392/v1

Version of Record: A version of this preprint was published at Natural Hazards on April 3rd, 2023. See the published version at https://doi.org/10.1007/s11069-023-05933-y.

Abstract

This study proposes a new model for flood inundation modeling using the Raster-based Probability Flood Inundation Model (RProFIM) approach. The flood modeling was carried out based on the landuse/landcover (LULC) change scenario and the difference in return periods in the study area. The aims of this study were: a) to estimate the volume of discharge in the LULC change scenario between 1990 and 2050 and the difference in return periods between 2 and 100 years; b) to create and produce flood inundation maps using the RProFIM approach; and c) to analyse flood damage assessment based on the results provided by overlaying LULC data with flood inundation maps. In general, the flood probability modeling generated by RProFIM provided the same pattern and conditions it was shown by reference data. The results found several potential areas in Citarum watershed, West Java-Indonesia which are likely to be flooded based on the RProFIM approach in the Districts of Margaasih, Kutawaringin, Margahayu, Katapang, Dayeuhkolot, and Baleendah. Flood damage assessment by the flood scenario with a return period of 2–100 years and changes in LULC in the range of 1990–2050, shows that the largest estimated loss based on market value is on built-up land and agriculture. This research is expected to be used as one of the considerations in managing environmental problems in overcoming flooding in the study area.

Introduction

Flood is one of the most frequent hydrometeorological disasters in Indonesia. There were around 10,438 flood events from 1815 to 2019. In 2021, there were 1,518 flood events resulted in 132 deaths and 782,054 people displaced (Fitriyani et al. 2021; Yulianto et al. 2022). Furthermore, the impact of flooding has also paralysed activities in several sectors such as infrastructure, productive economy, social facilities in the affected area and its surroundings (Akhmadi et al. 2018). Static and dynamic natural conditions can cause flooding. In static conditions, flooding can occur due to geographical, topographical, and geometric conditions of river channels, reservoirs, drainages that cause water overflow or inundation due to the limited capacity of the water body (Sastrodiharjo 2012; BNPB 2016). In dynamic conditions, flooding is caused by high rainfall, damming from the sea or tides occurring in the main river, land subsidence, river silting because of sedimentation, and also human activities that have a role on changes in LULC, such as deforestation, urbanisation, agricultural intensification and others (Yulianto et al. 2016; Yulianto et al. 2020; Winkler et al. 2021; Abebe et al. 2022).

LULC has an essential role in maintaining water balance, water quality and living organisms within a watershed. Changes in LULC occur dynamically and are complex, influenced by natural and anthropogenic factors. These changes are the result of the process of the interaction between humans and the environment, which requires land to meet the needs of life (Nagaraju et al. 2014; Sibanda and Ahmed 2020; Tahiru et al. 2020; Nahib et al. 2021). Changes in LULC have a significant impact on environmental issues, climate change, and natural ecosystem conditions and can also determine the level of flood risk within the watershed. These will affect the condition of surface runoff due to increasing rainfall intensity. The higher the surface runoff, the higher the flood risk level in the watershed (Szwagrzyk

et al. 2018; Chaudhary and Pandey 2022). Land degradation within the watershed can also affect the level of flooding due to changes in LULC. This is caused by changes in vegetation cover into built-up areas and results in a decrease in environmental quality that affects the hydrological characteristics of a watershed and has an impact on the high surface runoff (Ahmad et al. 2017; Trevisan et al. 2020).

The increasing development of GIS technology opens opportunities as a tool in spatial mapping, surface runoff distribution, and hydrological modelling that can be integrated with remote sensing data (Thakur et al. 2017). The dynamics of LULC changes can be monitored and mapped using multi-temporal remote sensing data (Zoungrana et al. 2015; Roy and Inamdar 2019; Abebe et al. 2021). Furthermore, the LULC information can be used as an input to estimate the runoff distribution (Rawat and Singh 2017; Zhang et al. 2022). Several studies related to this, QSWAT model (Tanksali and Soraganvi 2021); MIKE 11 NAM (Aredo et al. 2021); RHESSys (Mishra et al. 2021); the hydrodynamic model, HEC-RAS, and HEC-Geo RAS (Abdella and Mekuanent 2021); the RRI model (Nguyen et al. 2021); GeoWEPP and CLIGEN models (Singh et al. 2020); FLO-2D and HAND models (Komolafe et al. 2020); the SWMM model (Arjenaki et al. 2021).

Moreover, the results of surface runoff modelling can be used as input in flood modelling. Flood modellings can be developed from several approaches, based on planar models and hydrodynamic models (Ward, De Moel, et al. 2011). Planar models are a static flood modellings, such as research conducted by Marfai et al. (2008) and Ward, Marfai, et al. (2011) using an iterative model; Yulianto et al. (2016) using Monte Carlo; and Ward, De Moel, et al. (2011) using the Floodscanner model. Meanwhile, the hydrodynamic models are dynamics flood modeling, such research conducted by Afshari et al. (2018) using AutoRoute, HAND and HEC-RAS 2D; Giustarini et al. (2015) using PDWC2012; Arrault et al. (2016) used a 2-D shallow-water numerical model; Wing et al. (2019) using the 2-D hydrodynamic model and LISFLOOD-FP model; Fleischmann et al. (2019) using Large-scale hydrologic-hydrodynamic models and MGB models; Li et al. (2009), Lin et al. (2006), Liu at al. (2015), and Timbadiya et al. (2015) using 1D and 2D coupled hydrodynamic models; Pathan (2019) using GIS, HEC-RAS 1D and HEC-Geo RAS models; Huthoff et al. (2013), and Musa et al. (2015) using a 2D SOBEK hydrodynamic model; and Astuti (2017) using SWAT model.

In addition, several studies have also used the results of flood modelings to analyse the flood damage assessment, as previously performed by Velasco et al. (2015) to estimate the direct tangible damages based on the flood depth and new stage damage curves; Amirebrahimi et al. (2016) for microscale flood damage assessment and visualisation based on BIM-GIS integration; Amadio et al. (2016) to estimate economic damage based on the analysis of stage-damage curve models as a function of the characteristics of flood depth and land use; Chen et al. (2016) for calculate the direct tangible damage, the risk to life, and the health impact of individual flood events based on GIS-based tools; Choi et al. (2006) for the flood damage assessment in a building scale based on the multi-dimensional flood damage analysis (MD-FDA); Shrestha et al. (2019) for flood damage to rice crops based on the flood damage function which consists of flood depth, duration, and the growth stage of rice plants; Romali and Yusop (2020) for estimating the flood damage and risk assessment for urban areas based on the

combination of flood hazard (flood characteristics), exposure (value of exposed elements), and vulnerability (flood damage function curve).

The study area is located in the upstream Citarum watershed, West Java, Indonesia (Fig. 1), with a long flood history. Several studies showed that changes in LULC cause the increasing frequency of flooding in the study area. These changes occurred in the upstream area, which was previously a vegetated area then changed to built-up land (Tanika et al. 2020; Yulianto et al. 2020; Fadhil et al. 2021; Hudoso et al. 2021; Atharinafı and Wijaya 2021). Previous studies on the impact of LULC changes on surface runoff and flood modelling in the study area have also been carried out by several researchers with different methods. Dasanto et al. (2014a) has conducted research related to changes in forest cover on flood characteristics. The HEC-RAS model approach, integrated with GIS, is used to estimate and map inundation distribution in the study area. Siregar (2018) also uses the same approach to analyse the impact of the LULC change in 2001 and 2010 on flood conditions in urban areas. The modelling was carried out using HEC-RAS to describe flood inundation urban areas. Dasanto et al. (2014b) used a direct runoff (DRO) approach to determine adequate rainfall that caused flooding and GIS techniques to map the flood-prone areas. Nastiti et al. (2015) applied the rainfall-runoff-inundation (RRI) model for flood modelling in the study area. Siswanto (2020) has researched the impact of climate and LULC changes on the hydrological process and their relationship with historical and future changes by using spatial modelling. TETIS model has been applied to simulate the water and sediment cycle through the unit cell as process-based, which requires hydrometeorological time series and spatial map data. Fitriana (2020) has used MIKE FLOOD to conduct a flood vulnerability assessment based on numerical modelling. Fadhil et al. (2021) have conducted research related to analysing the effect of changes in LULC on hydrological characteristics in the study area. The hydrological response analysis was carried out using the flow regime coefficient approach and the annual flow coefficient to assess the effect of fluctuations in river discharge based on rainfall in the watershed area.

The implementation of the flood models in the study area is mainly done based on hydrodynamic models based on various methods that have been used in previous studies. Ward, Marfai et al. (2011) stated that there are limitations to use hydrodynamic modelling for inundation modelling, requiring complex input parameters and a long computational time to produce inundation characteristics in one flood event. This study is a follow-up study related to the spatial and temporal distribution of estimated surface runoff caused by LULC changes in the study area that has been done previously by Yulianto et al. (2022). The novelty of this study is related to flood inundation modelling using an RProFIM approach based on the scenarios of LULC change and return periods differences in the study area. RProFIM is a new raster-based model developed in this study for flood inundation probability modelling. The development of the RProFIM model was carried out by combining the concept of inundation probability from the Monte Carlo algorithm with the approximation formula. Several research objectives were made to run the model and its implementation to analyse the flood damage assessment in the study area.

The objectives of this study were: (a) to estimate the volume of discharge in the scenario of LULC changes ranging from 1990 to 2050 and differences in return periods ranging from 2 to 100 years; (b) to

create and produce flood inundation maps using an RProFIM approach; (c) to analyse the flood damage assessment based on the results of overlaying LULC data and flood inundation maps. It is aimed to reduce the impact of losses from flooding, and to support sustainable environmental management. Prevention, handling, and improving environmental problems and conditions are essential. The results of this study are expected to be used as one of the considerations in efforts to manage environmental problems in overcoming floods in the study area.

The structure of this paper is started with an introduction that explains in detail the state of the art of the research and the novel approach to mapping flood inundation. The next part is methods consisting of LULC and RProFIM in detail. The following part is the results that describe the scenario of the data processing experiment conducted in the study area and its result. Further analysis of the result compared to the recent works of literature and its theories are reported in the part of the discussions. The final part of the paper is the conclusions that summarize all the contents of this paper.

Methods

In this study, an overview of the methods can be presented in Fig. 2. There were three stages of research that are interrelated and used to answer the objectives and obtain research results. In the first stage, the estimated discharge for different return periods (ranging from 2 to 100 years) with the LULC change scenario (ranging from 1990 to 2050) scenario was calculated (Fig. 2a). In the second stage, flood inundation modelling was carried out using an RProFIM approach to obtain a map of the probability of inundation (Fig. 2b). In the third stage, flood damage assessment analysis was carried out by overlaying LULC data and flood inundation probability maps (Fig. 2c). The methodological stages of this study in more detail can be described in below sections.

Estimated discharge for different return periods and scenario LULC change

The estimated discharge Q in this research is based on a rational model approach formulated in equations (1–2) (Schwab et al., 1981; Alijani et al., 2016). Estimated runoff coefficient values, C are obtained based on the analysis and the input table of surface runoff coefficient values from various variations and types of LULC. LULC data in 1990, 2003, 2016 and predictions in 2025 and 2050 were obtained based on research conducted by Yulianto et al. (2019); Yulianto et al. (2020); Yulianto et al. (2022). The LULC data is a product of the results of analysis and digital classification of remote sensing data that can be presented in Fig. 3. Multi-temporal Landsat data with TM, ETM + and OLI/TIRS sensors were used to generate product and LULC information in 1990, 2003, 2016, respectively. Furthermore, LULC data predictions for 2025 and 2050 were obtained based on simulations using the Cellular Automata Markov (CA-Markov) model. There were 7 (seven) classes in the LULC data used in this study (Table 1), consisting of built land, primary forest, secondary forest and mix garden, plantation, wet agriculture land, dryland farming, and waterbody. The process estimates of runoff coefficient value C can be obtained by performing a communal table or open attribute table on the LULC vector data and an information table on

the surface runoff coefficient value for each variation and type of LULC. The estimates of runoff coefficient value for each LULC spatially can be presented in Fig. 4.

Table 1
Description of the LULC type and the surface runoff coefficient value used in this study

(Source and modified from Schwab et al. 1981; Alijani et al. 2016; Yulianto et al. 2019; Yulianto at al. 2020; Yulianto et al. 2022)

Class	LULC type	Description	Surface runoff coefficient value
1	Built-up land	Residential, commercial, industrial, villages, settlements, transportation infrastructure, and others.	0.60
2	Primary forest	The natural forest that has not been disrupted by human exploitation.	0.01
3	Secondary forest and mixed garden	Industrial plantation forest, garden plants, coconut, fruits, and others.	0.03
4	Plantation	Observation land, plantation of tea, palm, rubber, teak, and others.	0.40
5	Wet agriculture	Lands that require water for planting patterns, irrigated rice fields, rice terraces, and others.	0.15
6	Dryland farming	Land requires little water for cropping, fields, moor, and others.	0.10
7	Waterbody	Water resources, rivers, reservoirs, ponds, and others	0.05

$$Q = C.I.A$$

1

$$C = \frac{\sum A1.C1 + A2.C2 + A3.C3 + \cdots + An.Cn}{\sum A1 + A2 + A3 + \cdots + An}$$

2

Where Q is the peak flow in meters cubic per second, C is the surface runoff coefficient, I is the average rainfall intensity in meters per hour, A is the watershed area in square kilometres. (1, 2, 3, …, n is the LULC class ID).

Estimates of rainfall intensity I for 2, 5, 10, 25, 50, 100 years return periods in each sub-watershed was obtained based on research conducted by Fitriana (2020). The value of the design rainfall at various return periods was obtained from calculating the probability distribution of rainfall using the Gumbel method. Daily rainfall data for a period of 20 years (1999 to 2019) contained in 3 (three) locations of rainfall stations. They spread over 8 (eight) sub-watersheds (Cihaur, Cikapundung, Cikeruh, Ciminyak,

Cirasea, Cisangkuy, Citarik, Ciwidey) which were used as input to analyse the maximum daily rainfall and rainfall intensity return periods. Furthermore, the estimated of rainfall intensity for 2, 5, 10, 25, 50, 100 years return periods in each sub-watershed in the study area can be presented in Table 2.

Table 2
Estimates of rainfall intensity for 2, 5, 10, 25, 50, 100 years return periods in each sub-watershed in the study area

(Source and summarised from Fitriana 2020)

No	Sub-watershed	I-2RP	I-5RP	I-10RP	I-25RP	I-50RP	I-100RP
1	Cihaur	79.73	107.97	126.66	150.28	167.81	185.2
2	Cikapundung	79.73	107.97	126.66	150.28	167.81	185.2
3	Cikeruh	81.68	106.67	123.21	144.12	159.63	175.02
4	Ciminyak	87.02	108.25	123.55	139.1	160.33	177.61
5	Cirasea	87.93	113.07	129.7	150.73	166.33	181.82
6	Cisangkuy	87.02	108.25	123.55	139.1	160.33	177.61
7	Citarik	89.81	115.58	132.63	154.19	170.18	186.05
8	Ciwidey	87.02	108.25	123.55	139.1	160.33	177.61

Description: I-2RP is rainfall intensity (in mm) for 2-year return periods, I-5RP is for 5-year return periods, I-10RP is for 10-year return periods, I-25RP is for 25-year return periods, I-50RP is for 50-year return periods, I-100RP is for 100-year return periods.

The estimation of watershed and sub-watershed area A were carried out using an open attribute table and the calculated geometry on the vector data for watershed and sub-watershed boundaries in the study area. The data was obtained from The Ministry of Environment and Forestry (KLHK), a government ministry in the Republic of Indonesia.

Raster-based Probability Flood Inundation Model (RProFIM)

RProFIM is a novelty raster-based model developed in this study for flood inundation probability modelling. This model is static, not a dynamic model with a simple zero-dimensional planar-based approach. This model is used to overcome the complexity of the 2-D hydrodynamic model with various input parameters and requires a long computational time to produce an inundation model in a flood event. The development of the RProFIM model was carried out by combining the concept of inundation probability from the Monte Carlo algorithm with the approximation formula. The Monte Carlo algorithm was developed by Felpeto (2007) which is presented in equations (3–5). Meanwhile, the approximation formula was developed by Zhu (2010) which is presented in equations (6–7). The application and use of the Monte Carlo algorithm have been previously carried out by Yulianto et al. (2014) and Yulianto et al. (2016) to simulate inundation probabilities. Meanwhile, the approximation formula has been

implemented previously by Seniarwan et al. (2013); Yulianto et al. (2016) to simulate the inundation model.

$$P_i = \frac{\Delta h_i}{\sum_{j=1}^{8} \Delta h_j}$$

3

$$\Delta h_i = h_0 + h_c - h_i; if\,(h_0 + h_c + h_i) > 0$$

4

$$\Delta h_i = 0; if\,(h_0 + h_c + h_i) \leq 0$$

5

$$f\,(H) = Q - V$$

6

$$V = \sum_{k=1}^{m} A.\,h_c$$

7

$$f\,(H) = Q - \sum_{k=1}^{m} A.\,(H_k - (E_k)$$

8

Where: P_i is the flood inundation probability. h_i is the topography that represented by the hight value from Digital Elevation Model (DEM) data h with located in the cells i and j, ($i = 0$ and $j = 1, 2, 3, \ldots, 8$). Δh is the hight difference between the cell wit a cell-neighbourhood. h_c is the height correction. $f\,(H)$ is the equation function to analyse height of flood inundation H that is based on the ratio between volume topography V and volume flood Q. H_k is the accumulation of flood inundation height h_c and DEM elevation E_k in unit pixels k, ($k = 1, 2, 3, \ldots, n$). m is the number of unit pixels iterations. A is the unit pixels area.

Several flood modelling scenarios using RProFIM were run and carried out to determine whether there was an effect of LULC change on flood distribution in the study area. The primary input used to run this model is a raster-based DEM, and the results of the calculation of the value of the volume discharge at each sub-watershed outlet in the study area. The DEM data used in this study was the *DEM Nasional* (DEMNAS) obtained from the Geospatial Information Agency (BIG) in the Republic of Indonesia. The DEMNAS was built from several data sources consisting of IFSAR data with a resolution of 5 m,

TERRASAR-X with a resolution of 5 m, and ALOS PALSAR with a resolution of 11.25 m, and by adding the mass point of stereo-plotting results. DEMNAS has a spatial resolution of 0.27-arcsecond or about 8 m, with a vertical datum of EGM2008 (https://tanahair.indonesia.go.id/demnas/#/). The scenario consists of flood modelling for each LULC change in 1990, 2003, 2016, 2025, 2050 in return periods 2, 5, 10, 25, 50, 100 years. The model's output is inundation maps that show the potential and probability of flood inundation per grid-cell that has been resized with a grid size of 10 m * 10 m.

Flood damage assessment

Analysis of flood damage assessment in this study was carried out by overlaying LULC data and probability of flood inundation map. The analysis results can describe the overall conditions of the impact of inundation flooding in the study area. Furthermore, these results are used to determine flood damage assessment, which is based on the calculation of market value. Market value to determine flood damage assessment refers to research conducted by Marfai and King (2008), Ward, Marfai, et al. (2011), and Yulianto et al. (2016) which assumes that the market value of assets in the research area has the same value for the areas of Jakarta, Semarang and Manado, Indonesia. The estimated value of assets for built-up land (settlement and industrial) is €1.2 million per hectare. Meanwhile, for agriculture (wet agriculture and dryland farming), secondary forest and mixed garden, and plantation is €80,000 per hectare, and also for open area and water body is €1,700 per hectare. In addition, the results of mathematical model equations were also obtained that can be used to predict the estimated area of the impact of inundation floods in the next few years.

Results

Estimated discharge for different return periods and LULC change scenarios

Estimated discharge calculations were carried out in each sub-watershed in the study area, namely: Cihaur, Cikapundung, Cikeruh, Ciminyak, Cirasea, Cisangkuy, Citarik, and Ciwidey. The results of estimated discharge for different return periods (in the range of 2–100 years) and for scenario LULC change (in the range of 1990–2025) based on a rational model approach are presented in Table 3–7. Based on Tables 3–7, it is shown that the change in LULC had an effect on the estimated volume of discharge produced based on the rational model. It was also assumed that the value of rainfall intensity and area in each sub-watershed in the study area for a return period of 2–100 years was constant. The change in LULC had an effect on the coefficient value of each LULC class. The wider the changes that occur with the increase in built-up land, the higher the coefficient value and increases the estimated volume of discharge in each sub-watershed in the study area. It is certainly related to hydrological conditions, soil hydrological conditions and soil moisture conditions during precipitation of the drainage basin. The results of this study show that the peak discharge is sensitive to changes in LULC. The comparison of the effect of changing LULC on discharge at various return periods in this study area is presented in Fig. 5. It can be illustrated that, in general, the result of the calculation of the largest estimated discharge is the

Cikapundung sub-watershed. Meanwhile, the smallest estimated discharge calculation is the Ciwidey sub-watershed. This condition is caused by differences in land use, water use, pollution, and the level of erosion in the two locations. The increase in the calculation of the estimated discharge for each sub-watershed in the study area (Fig. 5) is influenced by the intensity of the rainfall which continues to increase every year in each return period (Table 2). In addition, the effect of LULC changes can contributes to the spatial distribution of runoff coefficient values (Fig. 4), and has an impact on increasing the calculation of the estimated discharge (Fig. 5).

Table 3
Summary of the calculation results of the estimated discharge for scenario LULC in 1990 and return periods in 2, 5, 10, 25, 50, 100 years in the study area

No	Sub-watershed	Q-2RP	Q-5RP	Q-10RP	Q-25RP	Q-50RP	Q-100RP
1	Cihaur	2,840	3,846	4,511	5,353	5,977	6,597
2	Cikapundung	5,110	6,920	8,118	9,632	10,756	11,871
3	Cikeruh	1,442	1,883	2,175	2,544	2,818	3,090
4	Ciminyak	1,472	1,831	2,090	2,354	2,713	3,005
5	Cirasea	2,758	3,547	4,068	4,728	5,217	5,703
6	Cisangkuy	2,134	2,655	3,030	3,412	3,932	4,356
7	Citarik	1,876	2,415	2,771	3,222	3,556	3,888
8	Ciwidey	763	949	1,083	1,219	1,406	1,557

Description: Q-2RP is estimated discharge (in 1,000 x m^3) for 2-year return periods, Q-5RP is for 5-year return periods, Q-10RP is for 10-year return periods, Q-25RP is for 25-year return periods, Q-50RP is for 50-year return periods, Q-100RP is for 100-year return periods.

Table 4
Summary of the calculation results of the estimated discharge for scenario LULC in 2003 and return periods in 2, 5, 10, 25, 50, 100 years in the study area

No	Sub-watershed	Q-2RP	Q-5RP	Q-10RP	Q-25RP	Q-50RP	Q-100RP
1	Cihaur	3,688	4,995	5,860	6,952	7,763	8,568
2	Cikapundung	5,832	7,897	9,264	10,992	12,274	13,546
3	Cikeruh	1,778	2,322	2,683	3,138	3,476	3,811
4	Ciminyak	1,869	2,325	2,654	2,988	3,444	3,815
5	Cirasea	3,180	4,090	4,691	5,452	6,016	6,576
6	Cisangkuy	2,614	3,252	3,712	4,179	4,817	5,336
7	Citarik	2,064	2,657	3,049	3,545	3,912	4,277
8	Ciwidey	1,098	1,366	1,559	1,755	2,023	2,241

Description: Q-2RP is estimated discharge (in 1,000 x m^3) for 2-year return periods, Q-5RP is for 5-year return periods, Q-10RP is for 10-year return periods, Q-25RP is for 25-year return periods, Q-50RP is for 50-year return periods, Q-100RP is for 100-year return periods.

Table 5 Summary of the calculation results of the estimated discharge for scenario LULC in 2016 and return periods in 2, 5, 10, 25, 50, 100 years in the study area

No	Sub-watershed	Q-2RP	Q-5RP	Q-10RP	Q-25RP	Q-50RP	Q-100RP
1	Cihaur	4,513	6,112	7,170	8,507	9,499	10,484
2	Cikapundung	6,984	9,457	11,094	13,164	14,699	16,222
3	Cikeruh	2,315	3,023	3,492	4,085	4,525	4,961
4	Ciminyak	2,030	2,525	2,882	3,245	3,741	4,144
5	Cirasea	3,768	4,845	5,558	6,460	7,128	7,792
6	Cisangkuy	3,401	4,231	4,829	5,437	6,266	6,942
7	Citarik	2,217	2,854	3,275	3,807	4,202	4,594
8	Ciwidey	1,272	1,582	1,806	2,033	2,343	2,596

Description: Q-2RP is estimated discharge (in 1,000 x m^3) for 2-year return periods, Q-5RP is for 5-year return periods, Q-10RP is for 10-year return periods, Q-25RP is for 25-year return periods, Q-50RP is for 50-year return periods, Q-100RP is for 100-year return periods.

Table 6
Summary of the calculation results of the estimated discharge for scenario LULC in 2025 and return periods in 2, 5, 10, 25, 50, 100 years in the study area

No	Sub-watershed	Q-2RP	Q-5RP	Q-10RP	Q-25RP	Q-50RP	Q-100RP
1	Cihaur	5,016	6,793	7,969	9,455	10,558	11,653
2	Cikapundung	7,652	10,363	12,156	14,424	16,106	17,775
3	Cikeruh	3,262	4,301	4,989	5,859	6,504	7,143
4	Ciminyak	2,687	3,436	3,958	4,538	5,173	5,723
5	Cirasea	3,994	5,194	5,987	6,991	7,736	8,475
6	Cisangkuy	3,358	4,271	4,911	5,611	6,410	7,094
7	Citarik	3,158	4,122	4,759	5,565	6,163	6,757
8	Ciwidey	1,813	2,349	2,717	3,141	3,563	3,939

Description: Q-2RP is estimated discharge (in 1,000 x m^3) for 2-year return periods, Q-5RP is for 5-year return periods, Q-10RP is for 10-year return periods, Q-25RP is for 25-year return periods, Q-50RP is for 50-year return periods, Q-100RP is for 100-year return periods.

Table 7
Summary of the calculation results of the estimated discharge for scenario LULC in 2050 and return periods in 2, 5, 10, 25, 50, 100 years in the study area

No	Sub-watershed	Q-2RP	Q-5RP	Q-10RP	Q-25RP	Q-50RP	Q-100RP
1	Cihaur	6,472	8,764	10,281	12,199	13,622	15,033
2	Cikapundung	9,082	12,299	14,428	17,118	19,115	21,096
3	Cikeruh	4,529	5,993	6,962	8,187	9,096	9,998
4	Ciminyak	4,068	5,241	6,052	6,971	7,924	8,764
5	Cirasea	5,128	6,705	7,749	9,069	10,048	11,020
6	Cisangkuy	4,578	5,875	6,776	7,786	8,863	9,805
7	Citarik	4,312	5,660	6,551	7,678	8,515	9,344
8	Ciwidey	3,382	4,387	5,077	5,873	6,659	7,363

Description: Q-2RP is estimated discharge (in 1,000 x m^3) for 2-year return periods, Q-5RP is for 5-year return periods, Q-10RP is for 10-year return periods, Q-25RP is for 25-year return periods, Q-50RP is for 50-year return periods, Q-100RP is for 100-year return periods.

Raster-based Probability Flood Inundation Model (RProFIM)

The results of several flood modelling scenarioswere accomplished and carried out using RProFIM to determine whether there was an effect of LULC change on flood distribution in the study area which can be presented in Figs. 6–10. The results of RProFIM based on the LULC scenario for 1990, 2003, 2016, 2025, and 2050 with their variation of return periods in the study area can be presented in Fig. 6, 7, 8, 9, and 10, respectively. The flood distribution generated from RProFIM can be described spatially based on the probability value. This value has a range from 0 to 1. A value of 0 indicates a low potential for possible flooding. Whereas, a value of 1 indicates a high spatial probability of flooding. The area of the flood inundation probability distribution was obtained based on each LULC change scenario, and the variation of the return period which was influenced by the number of input discharge estimates at each sub-watershed outlet in the study area. The higher the estimated discharge volume included in the RProFIM at each sub-watershed outlet, the wider the possible distribution of inundation. The example of visual magnification of the flood inundation model based on the LULC scenario in 2050 and a return period of 100 years, which is the result of overlaying RProFIM with a mosaic of SPOT 6/7 satellite imagery in 2020 from SPACeMAP LAPAN in Margaasih and Kutawaringin districts, are presented in Fig. 11. Meanwhile, in the Margahayu and Katapang districs are presented in Fig. 12, and also in the Dayeuhkolot and Baleendah districts are presented in Fig. 13. Figure 11–13 show the possible flood inundation visually overlaid with high resolution satellite imagery. These results also show the distribution of some areas that are inundated by floods. Some of these have an impact on built-up land (residential and industrial), agricultural land (wet agriculture and dryland farming), secondary forest and mixed garden, and plantation.

Flood damage assessment

Overlaid data and flood inundation probability map were used to determine the area affected by flood in the study area. The results described the overall conditions of the impact of flood inundation in the study area. The results of area affected by flood based on overlay of flood inundation map with LULC in various return periods are presented in Fig. 14. Based on Fig. 14, it can be illustrated that the areas affected by flooding are dry farming in each return period, followed by settlements and wet agriculture based on various scenarios.

Discussion

The effectiveness of the watershed function in maintaining a stability of the water balance and hydrological conditions at the landscape level is influenced by climate change and land use change. Integrated watershed planning efforts are needed in its management to regulate the allocation and utilization in the area. Assessing the hydrological function of the watershed is important as an initial step in watershed planning which aims to determine the condition of the watershed. So, it can be seen immediately that the watershed is in a degraded condition or has improved its watershed function. This study has produced an estimate for the calculation of the volume of discharge in the LULC changes scenario in 1990 until 2050, and its comparison in the 2–100 years return period scenario. The results of the estimated discharge calculations are used as input to create and produce probability of flood

inundation maps using an RProFIM approach. Furthermore, the results of the LULC overlay with flood inundation map are used for analysis of flood damage assessment. The discussion section of this study focuses the importance of modeling to assess the hydrological function of the watershed. Focuses on the analysis and comparison of results related to previous research efforts in assessing the function and hydrological conditions of the watershed in the study area. The comparison includes the estimation results of the discharge volume calculation, the results of flood inundation probability modeling maps, flood damage assessment analysis, limitations, and future research directions.

The importance of modeling to assess the hydrological function of the watershed

The importance of modeling to assess the hydrological function of the watershed is mainly carried out to determine the current conditions in the field. It is also useful for simulating mitigation efforts in various scenarios required for the restoration of watershed conditions. Several studies have applied various modeling techniques to assess watershed conditions using different methods in the study area. Tanika et al. (2020) had simulated the impact of land cover and climate change with the GenRiver Model in the study area. The simulation model was used to assess the hydrological conditions of the watershed and project its impacts due to land and climate change. The results of model simulations under conditions in 2012–2018 showed that on average 37% of the rainfall that falls in the Upper Citarum watershed becomes run-off, 7% becomes sub-surface flow, and 20% becomes base flow. Based on the simulation results on the extreme negative scenario, it shows that the degraded condition of the Upper Citarum watershed with the dominance of open land has the potential to increase surface runoff up to 70% of the rainfall. The existence of efforts to restore land cover with reforestation activities in extreme positive scenarios can reduce surface runoff to up to 20% of the total rainfall. The increase in rainfall intensity is also positively correlated with the increase in runoff in the study area. Thus, efforts are needed to increase the area of vegetated land that can be a buffer against changes in rainfall intensity. Listyarini et al. (2018) utilised the HEC-HMS model to simulate flood mitigation efforts in the study area. The modeling was carried out to study the characteristics of the flow discharge and to predict it through a hydrological model as a flood mitigation technique to predict flood discharge. There are 4 (four) flood mitigation scenarios used in this study, namely: a) the 1st scenario uses land use based on the spatial pattern in the West Java Province Spatial Plan for 2005–2025, b) the 2nd scenario uses the implementation of the plan. Forest and Land Rehabilitation techniques 2015–2029, c) the 3rd scenario uses land use by implementing an in situ flow control system and optimizing the function of water catchment areas, d) the 4th scenario using a combination of scenarios 1, 2, and 3. The simulation results of the HEC-HMS model with the application of various scenarios are able to reduce peak discharge in each sub-watershed. The results in the 1st, 2nd, 3rd, and 4th scenarios that can reduce peak discharge under actual conditions are 34.62%, 33.61%, 60.46%, and 61.69%, respectively. The decrease in peak discharge in scenarios 3 and 4 is caused by the increase in the area of water absorption by reforestation, and the application of infiltration wells. This can increase the retention ability which is large when it rains, and the rainfall does not immediately turn into runoff.

Comparison of results related to the estimated of the discharge volume

In addition to climate and rainfall factors, LULC changes are also one of the factors that contribute to the increase in flow rate in the study area. Atharinafi and Wijaya (2021) showed a change in LULC increased the surface runoff coefficient on the curve numbers during the 1999 and 2018 periods, which were 70.98 and 72.04, respectively. Meanwhile, the surface runoff has increased from 48.49 mm to 51.8 mm, assuming that the rainfall for 24 hours was 120 mm. These changes occurred in the upstream area, which was previously a vegetated area that changed to build up land. Tanika et al. (2020) stated that based on the latest simulations from 2019 to 2028, it showed that surface runoff will increase by 1% of the total rainfall for every conversion of 4,700 hectares of the vegetated land cover into open land. Yulianto et al. (2020) stated an increase in the built-up area of more than 11,000 hectares in the period 1990 to 2016. Fadhil et al. (2021) stated an increase of the built-up area by 11,305 hectares or around 39.7% from 2009 to 2018 and a decrease of forest cover by about 1,611 hectares or around 5.6%. Hudoso et al. (2021) also reported a 35% of decrease in vegetated land cover during the period 1989 to 2019. The estimation results of the calculation of the volume of discharge using the rational model in this study (Table 5–7), which are scenarios for each change in LULC from 1990 to 2050 show an increase in the volume of discharge in each sub-watershed in the study area. The same results were also found by Sipayung and Cholianawati (2011) that changes in land cover affect the hydrological conditions, microclimate, and water balance in the study area. The research was conducted based on the results of the analysis of the atmospheric model output, and it was estimated that there will be an increase in runoff in 2011–2019 in the study area. The results of the study also showed a correlation coefficient of 0.8 from the results of model calculations with observations in the study area. Sentosa et al. (2021) used the Soil Conservation Service-Curve Number (SCS-CN) method to estimate the runoff volume of the Cikeruh sub-watershed which is one of the sub-watersheds in the study area. The results of the study at the same location and year were used as a reference (obs). The results of the calculation of the correlation coefficient (R2) and Pearson's correlation coefficient (R) were 0.974 and 0.987, which indicates a positive correlation with our research using the rational method (model) to estimate runoff volume in the 2–100 year return period (Fig. 15a). Comparisons were also made based on the results of research conducted by Nuryono et al. (2015) in estimating the volume of runoff discharge in the Cisangkuy sub-watershed which is part of the sub-watershed in the study area. The results of comparisons that have been carried out using the rational method (model) with the log normal probability distribution (Obs) in Cisangkuy sub-watershed show a positive correlation with R2 and R values of 0.997 and 0.998 (Fig. 15b).

Comparison of results related to the flood modeling

Nastiti et al. (2015) used the RRI model for flood modeling and reproduced the 2010 major flood event in the study area. The study used 15 arc-second HydroSHEDS Digital Elevation Model (DEM) and satellite-based hourly rainfall data (GSMaP) as input, which were validated using daily observation data. The results of the study showed good agreements on the results of the flood simulation, but for the discharge simulation it showed some differences with the observation measurements due to the uncertainty factor

of the input data used. Siregar and Indrawan (2017) conducted 1-D and 2-D flood modeling using HEC-RAS which can be used to predict floods in 2007 and 2008 events in the study area. The same thing was also done by Siregar (2018) to conduct flood modeling and generate flood parameters in the form of water level and flood discharge in the scenario of extreme flood conditions in 2010 using numerical analysis Force2 programming and HEC-RAS in the study area. The research shows that the optimal design of flood modeling leads to the improvement of flood prevention structures. Based on the results of modeling using HEC-RAS for 2D modeling during the 2010 extreme flood events, it was shown that several locations in the study area were almost completely submerged by the overflow of the Citarum River. The results of these studies in producing flood modeling in the study area generally have the same pattern and conditions as the results of flood probability modeling using RProFIM which was carried out in this study. Several areas that have the potential and probability of being inundated during flooding based on the RProFIM approach include the Margaasih, Kutawaringin (Fig. 11), Margahayu, Katapang (Fig. 12), Dayeuhkolot, and Baleendah districts (Fig. 13).

Flood assessment analysis to estimate flood loss damage based on market value

The overlay result of the flood probability model from RProFIM with LULC was used to determine the extent of the flood impact from various conditions of variation in return periods (range 2–100 years) and LULC (range 1990–2050) in the study area (Fig. 14). Based on these results in various scenarios, it can be shown that in general the largest flood impact is on agricultural land and built-up land which continues to increase every year in the return period range of 2–100 years. Moe et al. (2018) stated that there were more than 6,000 houses and more than 3,500 people who were affected by the 21–25 February 2018 flood in the study area. The flood incident also affected 10 villages with a flood depth of 80–120 cm. The results of flood damage assessment based on overlay of flood inundation map with LULC in various return periods, which is based on the calculation of market value are presented in Fig. 16. The results of this study, which are modeled on a flood scenario with a return period of 2–100 years and changes in LULC in the range of 1990–2050, indicate that the largest estimated loss based on market value is in built-up land and agriculture. The results of flood damage assessment model for built-up land and agriculture in LULC scenarios ranging 1990–2050 are presented in Fig. 17. Fernandos et al. (2020) stated that the estimated level of loss in the study area was influenced by the type of LULC and the market value of each type of LULC. In addition, it is also affected by the extent of LULC affected by flooding. The results of this study indicate that in the flood hazard level scenario in the 25 year flood event return period, the largest flood losses have an impact on settlements, commercial/industrial, and agriculture areas. The impact of the flood losses was also presented by Muin et al. (2015) that the settlement sector and the agricultural sector have the largest losses as a result of the impact of the flood in the scenario of a 5–25 year return period. Furthermore, the results of mathematical model equations are obtained that can be used to predict the built-up flood damage assessment of the floods impact are presented in Table 8, and also for agriculture are presented in Table 9. The equations in Table 8 and Table 9can be used to estimate the impact of flood losses in the study area for several return periods in the scenario based on land change years in the built-up and agriculture sectors.

Table 8
The resulting mathematical model equations that can be used to predict the built-up flood damage assessment of the floods impact

LULC	Scenario (years)	Mathematical model equations
Built-up	1990	FDA_BU(1990) = 469,56 ln(nRT) + 191,57
Built-up	2003	FDA_BU(2003) = 502,68 ln(nRT) + 207,08
Built-up	2016	FDA_BU(2016) = 556,58 ln(nRT) + 191,07
Built-up	2025	FDA_BU(2025) = 585,76 ln(nRT) + 221,61
Built-up	2050	FDA_BU(2050) = 633,76 ln(nRT) + 230,62

Description: $\mathrm{FDA}_{\mathrm{BU}(1990)}$ is the built-up flood damage assessment for scenario in 1990, $\mathrm{FDA}_{\mathrm{BU}(2003)}$ for scenario in 2003. $\mathrm{FDA}_{\mathrm{BU}(2016)}$ for scenario in 2016. $\mathrm{FDA}_{\mathrm{BU}(2025)}$ for scenario in 2025. $\mathrm{FDA}_{\mathrm{BU}(2050)}$ for scenario in 2050. $\ln(\mathrm{nRT})$is the natural logarithm function for return period in $n-years$.

Table 9
The resulting mathematical model equations that can be used to predict the agriculture flood damage assessment of the floods impact

LULC	Scenario (years)	Mathematical model equations
Agriculture	1990	FDA_AG(1990) = 60,26 ln(nRT) + 15,59
Agriculture	2003	FDA_AG(2003) = 66,34 ln(nRT) + 17,44
Agriculture	2016	FDA_AG(2016) = 74,71 ln(nRT) + 20,87
Agriculture	2025	FDA_AG(2025) = 78,93 ln(nRT) + 22,15
Agriculture	2050	FDA_AG(2050) = 86,43 ln(nRT) + 24,43

Description: $\mathrm{FDA}_{\mathrm{AG}(1990)}$ is the agriculture flood damage assessment for scenario in 1990, $\mathrm{FDA}_{\mathrm{AG}(2003)}$ for scenario in 2003. $\mathrm{FDA}_{\mathrm{AG}(2016)}$ for scenario in 2016. $\mathrm{FDA}_{\mathrm{AG}(2025)}$ for scenario in 2025. $\mathrm{FDA}_{\mathrm{AG}(2050)}$ for scenario in 2050. $\ln(\mathrm{nRT})$is the natural logarithm function for return period in $n-years$.

Limitations and future research possible direction

There are several limitations in the implementation of this study that affect the results of this study. These limitations include several technical aspects, use of data, reference models, and also some assumptions used to carry out this study. The limitation in determining the estimated discharge volume in this study is that the data used as input for determining the intensity of rainfall in the 2-100 year return period still refers to the research conducted by Fitriana (2020). In addition, there are also limited references related to the research to determine the estimated distribution of the discharge volume in the study area. Efforts to compare the results of this study with the same research are constrained and can

only be carried out on two sub-watersheds in the research area, namely: Cikeruh and Cisangkuy. In future research, several uses of satellite-based rainfall data such as Himawari-8, TRMM, GSMaP, QMORPH, CHIRPS can be used as input for rainfall intensity data that has been calibrated with field observations. It can also be used as an alternative if rainfall measurement data are not available in the field. The rational model is used in this study to determine the estimated discharge volume. In future research, the use of other methods such as the SCS-CN, RRI, HEC-HMS and other models can be used as a comparison of the results of this study. The determination of the runoff coefficient value for each LULC class in this study was based on a modified surface runoff coefficient value table that referred to the study of Schwab et al. (1981), Alijani et al. (2016); Yulianto et al. (2019), Yulianto at al. (2020), and Yulianto et al. (2022). Field measurement efforts are needed in future research to be able to determine the actual value of the runoff coefficient for each LULC class in the research area. The LULC data used in this study has a resolution of 30 m, which is the product of a study conducted by Yulianto et al. (2019), Yulianto at al. (2020), and Yulianto et al. (2022). Utilization of high resolution satellite image data such as SPOT 6/7, Pleiades, Worldview is needed in future research, so that the LULC has more detailed information in determining the runoff coefficient. The DEM data used as one of the RProFIM inputs is DEMNAS data, which has been resized to a resolution gird of 10 m * 10 m. Detailed DEM efforts are needed in future research, one of which is using SPOT 6/7 stereo data to produce DEM data with higher spatial resolution. The limitation of the flood modeling carried out in this study is related to the probability of flood inundation that occurs in the study area. The probability value of the resulting flood inundation ranges from 0 (low) to 1 (high). Further algorithm development efforts are needed in future research to be able to determine other flood parameters such as flood depth, flood duration, and others. Determination of market value is still based on assumptions that refer to research conducted by Marfai and King (2007), Ward, Marfai, et al. (2011), and Yulianto et al. (2016). The prevailing market value in the study area is still assumed to have the same value as that found in the areas of Jakarta, Semarang, and Manado in Indonesia. There is a need for future research that specifically discusses determining market value due to flooding in the study area. Thus, the flood damage assessment calculations carried out in this study have results that are in accordance with current conditions in the field.

Conclusions

The importance of modeling to assess the hydrological function of the watershed is mainly carried out to determine the current conditions in the field. It is also useful for simulating mitigation efforts in various scenarios required for the restoration of watershed conditions. This study has produced the probability of flood inundation map based on RProFIM approach. The existence of a LULC change scenarios in 1990 to 2025 has had an impact on increasing the estimated discharge volume in each scenario of a return period of 2–100 years. The results of the estimated discharge volume for each scenario that are inlcuded into the RProFIM system have an influence on the probability of the resulting flood inundation. Flood modeling resulted in this study using RProFIM generally have the same pattern and conditions with the reference data. Several areas that have the potential and probability of being inundated during flooding based on the RProFIM approach include the Margaasih, Kutawaringin, Margahayu, Katapang,

Dayeuhkolot, and Baleendah districts. The overlay result of the flood probability model from RProFIM with LULC was used to determine the extent of the flood impact in the study area. It can be shown that in general the largest flood impact is on agricultural land and built-up land which continues to increase every year in the return period range of 2–100 years. Furthermore, the resulting mathematical model equations can be used to predict the built-up and agriculture flood damage assessment. These equations can be used to estimate the impact of flood losses in the study area for several return periods in the scenario based on land change years in the built-up and agriculture sectors. In future research, it is necessary to develop further reserch related to machine learning-based processing techniques that can be integrated in determining flood potential and assessing flood damage.

Declarations

Funding:

The study was funded by the National Innovation System Research Incentive (INSINAS) of 2021, the Ministry of Research Technology, and the Higher Education Republic of Indonesia. Contract number: 13/INS/PPK/E4/2021.

Acknowledgements:

This paper is a part of the study activities entitled "Integration of Remote Sensing Data for Flood Impact Analysis, Environmental Management and Disaster Mitigation in the Citarum Watershed, West Java Province, Indonesia". The study was funded by the National Innovation System Research Incentive (INSINAS) of 2021, the Ministry of Research Technology, and the Higher Education Republic of Indonesia. Contract number: 13/INS/PPK/E4/2021. The authors thank the anonymous reviewers for their efforts and constructive comments, which have allowed us to improve the manuscript.

Conflicts of Interest: The authors declare no conflict of interest.

References

1. Abdella K, Mekuanent F (2021) Application of hydrodynamic models for designing structural measures for river flood mitigation: the case of Kulfo River in southern Ethiopia. Modeling Earth Systems and Environment, *7*(4): 2779–2791. https://doi.org/10.1007/s40808-020-01057-5.
2. Abebe M, Legesse A, Gadisa F, Hussen M (2022) Challenges and Opportunities for the Agricultural Producers in Sinana District in Reflection of COVID-19 Pandemic. Advances in Agriculture. https://doi.org/10.1155/2022/4511995.
3. Afshari S, Tavakoly AA, Rajib MA, Zheng X, Follum ML, Omranian E, Fekete BM (2018). Comparison of new generation low-complexity flood inundation mapping tools with a hydrodynamic model. Journal of Hydrology, 556:539–556. https://doi.org/https://doi.org/10.1016/j.jhydrol.2017.11.036.

4. Ahmad S, Israr M, Yaseen A (2017) Land degradation a threat to sustainable rural development in Northern highlands of Pakistan.
5. Akhmadi, Rahmitha, Wahyu YFM (2018) Impact of Climate Change on Households in the Indonesian CBMS Area. The SMERU Research Institute, 8(3):281–288.
6. Alijani A, Ghadimvand NK, Aleali M, Espahbod MR, Meysami A (2016) Evaluating the Amount of Erodability and Sedimentation by Comparing Sediment Weight Model and PSIAC Experimental Model (Case Study: Lali Water Catchment, Khuzestan, Iran). Open Journal of Geology, 06(08):692–702. https://doi.org/10.4236/ojg.2016.68053.
7. Amadio M, Mysiak J, Carrera L, Koks E (2016) Improving flood damage assessment models in Italy. Natural Hazards, 82(3):2075–2088. https://doi.org/10.1007/s11069-016-2286-0.
8. Amirebrahimi S, Rajabifard A, Mendis P, Ngo T (2016) A framework for a microscale flood damage assessment and visualization for a building using BIM–GIS integration. International Journal of Digital Earth, 9(4):363–386. https://doi.org/10.1080/17538947.2015.1034201.
9. Aredo MR, Hatiye SD, Pingale SM (2021) Modeling the rainfall-runoff using MIKE 11 NAM model in Shaya catchment, Ethiopia. Modeling Earth Systems and Environment, *7*(4):2545–2551. https://doi.org/10.1007/s40808-020-01054-8.
10. Arjenaki MO, Sanayei HRZ, Heidarzadeh H, Mahabadi NA (2021) Modeling and investigating the effect of the LID methods on collection network of urban runoff using the SWMM model (case study: Shahrekord City). Modeling Earth Systems and Environment, 7(1):1–16. https://doi.org/10.1007/s40808-020-00870-2.
11. Arrault A, Finaud-Guyot P, Archambeau P, Bruwier M, Erpicum S, Pirotton M, Dewals B (2016) Hydrodynamics of long-duration urban floods: Experiments and numerical modelling. Natural Hazards and Earth System Sciences, 16(6): 1413–1429. https://doi.org/10.5194/nhess-16-1413-2016.
12. Atharinafı Z, Wijaya N (2021) Land use change and its impacts on surface runoff in rural areas of the upper citarum watershed (case study: Cirasea subwatershed). Journal of Regional and City Planning, 32(1):36–55. https://doi.org/10.5614/jpwk.2021.32.1.3.
13. BNPB (2016) Risiko Bencana Indonesia (Disasters Risk of Indonesia). (In Bahasa).
14. Chaudhary S, Pandey AC (2022) PCA driven watershed prioritization based on runoff modeling and drought severity assessment in parts of Koel river basin, Jharkhand (India). Water Supply, 22(2):2034–2054. https://doi.org/10.2166/ws.2021.297.
15. Chen AS, Hammond MJ, Djordjević S, Butler D, Khan DM, Veerbeek W (2016) From hazard to impact: flood damage assessment tools for mega cities. Natural Hazards, 82(2):857–890. https://doi.org/10.1007/s11069-016-2223-2.
16. Choi SA, Yi CS, Shim MP, Kim HS (2006) Multi-Dimensional Flood Damage Analysis: Principle and Procedure. Journal of Korea Water Resources Association, 39. https://doi.org/10.3741/JKWRA.2006.39.1.001.

17. Dasanto BD, Boer R, Pramudya B, Suharnoto Y (2014) Simple method for assessing spread of flood prone areas under historical and future rainfall in the upper citarum watershed. EnvironmentAsia, *7*(2): 79–86.
18. Dasanto BD, Pramudya B, Boer R, Suharnoto Y (2014) Effects of forest cover change on flood characteristics in the upper citarum watershed. Jurnal Manajemen Hutan Tropika, 20(3): 141–149. https://doi.org/10.7226/jtfm.20.3.141.
19. Fadhil MY, Hidayat Y, Baskoro DPT (2021) Identifikasi Perubahan Penggunaan Lahan dan Karakteristik Hidrologi DAS Citarum Hulu. Jurnal Ilmu Pertanian Indonesia, 26(2):213–220. https://doi.org/10.18343/jipi.26.2.213. (In Bahasa).
20. Felpeto A, Martí J, Ortiz R (2007) Automatic GIS-based system for volcanic hazard assessment. Journal of Volcanology and Geothermal Research, 166(2):106–116. https://doi.org/10.1016/j.jvolgeores.2007.07.008.
21. Fernandos, Tambunan MP, Marko K (2020) Loss levels regarding flood affected areas in the upper Citarum Watershed. IOP Conference Series: Earth and Environmental Science, 561(1). https://doi.org/10.1088/1755-1315/561/1/012027.
22. Fitriana HL (2020) Penilaian kerentanan banjir di DAS Citarum Hulu. Thesis S2. Universitas Indonesia. (In Bahasa).
23. Fitriyani J, Apriyadi RK, Winugroho T, Hartono D, Widana IDKK, Wilopo W (2021) Characteristics of Indonesia's disaster history for the period 1815–2019 based on the number of disasters, deaths, exposures and house damage due to disasters. PENDIPA Journal of Science Education 5(3):322-327, https://doi:10.33369/pendipa.5.3.322-327.
24. Fleischmann A, Paiva R, Collischonn W (2019) Can regional to continental river hydrodynamic models be locally relevant? A cross-scale comparison. Journal of Hydrology X, 3, 100027. https://doi.org/https://doi.org/10.1016/j.hydroa.2019.100027.
25. Giustarini L, Chini M, Hostache R, Pappenberger F, Matgen P (2015) Flood Hazard Mapping Combining Hydrodynamic Modeling and Multi Annual Remote Sensing data. Remote Sensing, 7:14200–14226. https://doi.org/10.3390/rs71014200.
26. Husodo T, Ali Y, Mardiyah SR, Shanida SS, Abdoellah OS, Wulandari I (2021) Perubahan lahan vegetasi berbasis citra satelit di DAS Citarum, Bandung, Jawa Barat. Majalah Geografi Indonesia 35(1):54-63, https://doi:10.22146/mgi.31217. (In Bahasa).
27. Komolafe A, Awe B, Olorunfemi IE, Oguntunde P (2020) Modelling flood-prone area and vulnerability using integration of multi-criteria analysis and HAND model in the Ogun River Basin, Nigeria. Hydrological Sciences Journal, 65. https://doi.org/10.1080/02626667.2020.1764960.
28. Li W, Chen Q, Mao J (2009) Development of 1D and 2D coupled model to simulate urban inundation: An application to Beijing Olympic Village. Chinese Science Bulletin, 54(9):1613–1621. https://doi.org/10.1007/s11434-009-0208-1.
29. Lin B, Wicks J, Falconer R, Adams K (2006) Integrating 1D and 2D hydrodynamic models for flood simulation. Proceedings of the Institution of Civil Engineers: Water Management, 159.

https://doi.org/10.1680/wama.2006.159.1.19.

30. Listyarini D, Hidayat Y, Tjahjono B (2018) Mitigasi Banjir Das Citarum Hulu Berbasis Model Hec-Hms. Jurnal Ilmu Tanah Dan Lingkungan, 20(1):40–48. https://doi.org/10.29244/jitl.20.1.40-48. (In Bahasa).
31. Liu Q, Qin Y, Zhang Y, Li Z (2015) A coupled 1D–2D hydrodynamic model for flood simulation in flood detention basin. Natural Hazards, 75(2):1303–1325. https://doi.org/10.1007/s11069-014-1373-3.
32. Marfai MA, King L (2008) Potential vulnerability implications of coastal inundation due to sea level rise for the coastal zone of Semarang city, Indonesia. Environmental Geology, 54(6):1235–1245. https://doi.org/10.1007/s00254-007-0906-4.
33. Marfai MA, King L, Sartohadi J, Sudrajat S, Budiani SR, Yulianto F (2008) The impact of tidal flooding on a coastal community in Semarang, Indonesia. Environmentalist, 28(3):237–248. https://doi.org/10.1007/s10669-007-9134-4.
34. Nuryono B, Ramdaniah D (2015) Analisis frekuensi debit banjir menggunakan metode probabilitas. Isu Teknologi STT Mandala. 10(2):25-38. (In Bahasa).
35. Nahib I, Ambarwulan W, Rahadiati A, Munajati SL, Prihanto Y, Suryanta J, Turmudi T, Nuswantoro AC (2021) Assessment of the impacts of climate and LULC changes on the water yield in the citarum River Basin, West Java Province, Indonesia. Sustainability (Switzerland), 13(7). https://doi.org/10.3390/su13073919.
36. Nastiti K, Kim Y, Jung K. an H. (2015). The Application of Rainfall-Runoff-inundation (RRI) Model for Inundation Case in Upper Citarum Watershed, West Java-Indonesia. Procedia Engineering, 125:166–172. https://doi.org/10.1016/j.proeng.2015.11.024.
37. Nguyen T, Nakatsugawa M, Yamada T, Hoshino T (2021) Flood Inundation Assessment in the Low-Lying River Basin Considering Extreme Rainfall Impacts and Topographic Vulnerability. Water, 13:896. https://doi.org/10.3390/w13070896.
38. Pathan AI (2019) A Combined Approach For 1-D Hydrodynamic Flood Modeling By using Arc-Gis, Hec-Georas, Hec-Ras Interface -A Case Study On Purna River Of Navsari City, Gujarat.
39. Rawat KS, Singh SK (2017) Estimation of Surface Runoff from Semi-arid Ungauged Agricultural Watershed Using SCS-CN Method and Earth Observation Data Sets. Water Conservation Science and Engineering, 1(4):233–247. https://doi.org/10.1007/s41101-017-0016-4.
40. Romali NS, Yusop Z (2021) Flood damage and risk assessment for urban area in Malaysia. Hydrology Research, 52(1):142–159. https://doi.org/10.2166/NH.2020.121.
41. Roy A, Inamdar AB (2019) Multi-temporal Land Use Land Cover (LULC) change analysis of a dry semi-arid river basin in western India following a robust multi-sensor satellite image calibration strategy. Heliyon, 5(4):e01478. https://doi.org/10.1016/j.heliyon.2019.e01478.
42. Seniarwan S, Baskoro DPT, Gandasasmita K (2013) Analisis Spasial Risiko Banjir Wilayah Sungai Mangottong Di Kabupaten Sinjai, Sulawesi Selatan. Jurnal Ilmu Tanah Dan Lingkungan, 15(1):39. https://doi.org/10.29244/jitl.15.1.39-44. (In Bahasa).

43. Sentosa AK, Asdak C, Suryadi E (2021) Estimasi Volume Limpasan dan Debit Puncak Sub DAS Cikeruh Menggunakan Metode SCS-CN (Soil Conservation Service-Curve Number). Jurnal Keteknikan Pertanian Tropis Dan Biosistem, 9(1):90–98. https://doi.org/10.21776/ub.jkptb.2021.009.01.10. (In Bahasa).
44. Schwab G et al. (1981) Soil and Water Conservation Engineering. John Wiley Inc., New York.
45. Shrestha B, Perera D, Kudo S, Miyamoto M, Yamazaki Y, Kuribayashi D, Sawano H, Sayama T, Magome J, Hasegawa A, Ushiyama T, Iwami Y, Tokunaga Y (2019) Assessing flood disaster impacts in agriculture under climate change in the river basins of Southeast Asia. Natural Hazards, 97. https://doi.org/10.1007/s11069-019-03632-1.
46. Sibanda S, Ahmed F (2021) Modelling historic and future land use/land cover changes and their impact on wetland area in Shashe sub-catchment, Zimbabwe. Modeling Earth Systems and Environment, 7:1–14. https://doi.org/10.1007/s40808-020-00963-y.
47. Sipayung SB, Cholianawati N (2011) Proyeksi Debit Aliran Permukaan Das Citarum Berbasis Luaran Model Atmosfer. Jurnal Sains Dirgantara, 8:115–128. (In Bahasa).
48. Siregar RI (2018) Numerical Analysis of Flood modeling of upper Citarum River under Extreme Flood Condition. IOP Conference Series: Materials Science and Engineering, 308(1). https://doi.org/10.1088/1757-899X/308/1/012023.
49. Siregar RI, Indrawan I (2017) Studi Komparasi Pemodelan 1-D (Satu Dimensi) Dan 2-D (Dua Dimensi) Dalam Memodelkan Banjir Das Citarum Hulu. Educational Building, 3(2):31–37. https://doi.org/10.24114/eb.v3i2.8255. (In Bahasa).
50. Szwagrzyk J, Maciejewski Z, Maciejewska E, Tomski A, Gazda A (2018) Forest recovery in set-aside windthrow is facilitated by fast growth of advance regeneration. Annals of Forest Science, 75. https://doi.org/10.1007/s13595-018-0765-z.
51. Tahiru AA, Doke DA, Baatuuwie BN (2020) Effect of land use and land cover changes on water quality in the Nawuni Catchment of the White Volta Basin, Northern Region, Ghana. Applied Water Science, 10(8):1–14. https://doi.org/10.1007/s13201-020-01272-6.
52. Tanksali A, Soraganvi V (2021) Assessment of impacts of land use/land cover changes upstream of a dam in a semi-arid watershed using QSWAT. Modeling Earth Systems and Environment, 7. https://doi.org/10.1007/s40808-020-00978-5.
53. Thakur JK, Singh SK, Ekanthalu VS (2017) Integrating remote sensing, geographic information systems and global positioning system techniques with hydrological modeling. Applied Water Science, 7(4):1595–1608. https://doi.org/10.1007/s13201-016-0384-5.
54. Timbadiya PV, Patel PL, Porey P (2015) A 1D–2D Coupled Hydrodynamic Model for River Flood Prediction in a Coastal Urban Floodplain. Journal of Hydrologic Engineering, 20:5014017. https://doi.org/10.1061/(ASCE)HE.1943-5584.0001029.
55. Trevisan D, Bispo P, Almeida D, Imani M, Balzter H, Moschini L (2020). Environmental vulnerability index: An evaluation of the water and the vegetation quality in a Brazilian Savanna and Seasonal Forest biome. Ecological Indicators, 112. https://doi.org/10.1016/j.ecolind.2020.106163.

56. Velasco M, Cabello A, Russo B (2015) Flood damage assessment in urban areas. Application to the Raval district of Barcelona using synthetic depth damage curves. Urban Water Journal, 13:1–15. https://doi.org/10.1080/1573062X.2014.994005.
57. Ward PJ, De Moel H, Aerts JCJH (2011) How are flood risk estimates affected by the choice of return-periods? Natural Hazards and Earth System Science, 11(12):3181–3195. https://doi.org/10.5194/nhess-11-3181-2011.
58. Ward PJ, Marfai MA, Yulianto F, Hizbaron DR, Aerts JCJH (2011) Coastal inundation and damage exposure estimation: A case study for Jakarta. Natural Hazards, 56(3):899–916.
59. Wing OEJ, Sampson CC, Bates PD, Quinn N, Smith AM, Neal JC (2019) A flood inundation forecast of Hurricane Harvey using a continental-scale 2D hydrodynamic model. Journal of Hydrology X, 4(August). https://doi.org/10.1016/j.hydroa.2019.100039.
60. Winkler K, Fuchs R, Rounsevell M, Herold M (2021) Global land use changes are four times greater than previously estimated. Nature Communications, 12(1):1–10. https://doi.org/10.1038/s41467-021-22702-2.
61. Siswanto SY, Francés F (2012) Impact of climate changes on water, flood and sediment cycles in asean tropical country. A case study in indonesian watershed using distributed modeling.
62. Tanika L, Lusiana B, Hendriatna A (2021) Simulating the effect of change in land cover and rainfall in Upper Citarum Watershed: calibration and sensitivity analysis of GenRiver model. Working paper no. 310. Bogor, Indonesia: World Agroforestry (ICRAF). https://doi.org/10.5716/WP20049.PDF.
63. Yulianto F, Khomarudin MR, Hermawan E, Nugroho NP, Chulafak GA, Nugroho G, Nugroho UC, Suwarsono, Fitriana HL, Priyanto E (2022) Spatial and temporal distribution of estimated surface runoff caused by land use/land cover changes in the upstream Citarum watershed, West Java, Indonesia. Journal of Degraded and Mining Lands Management, 9(2):3293–3305. https://doi.org/10.15243/jdmlm.2022.092.3293.
64. Yulianto F, Maulana T, Khomarudin MR (2019) Analysis of the dynamics of land use change and its prediction based on the integration of remotely sensed data and CA-Markov model, in the upstream Citarum Watershed, West Java, Indonesia. International Journal of Digital Earth, 12(10):1151–1176. https://doi.org/10.1080/17538947.2018.1497098.
65. Yulianto F, Nugroho UC, Nugroho NP, Sunarmodo W, Khomarudin MR (2020) Spatial-Temporal Dynamics Land Use/Land Cover Change and Flood Hazard Mapping in the Upstream Citarum Watershed, West Java, Indonesia. Quaestiones Geographicae, 39(1):125–146. https://doi.org/10.2478/quageo-2020-0010.
66. Yulianto F, Prasasti I, Pasaribu JM, Fitriana HL, Zylshal, Haryani NS, Sofan P (2016) The dynamics of land use/land cover change modeling and their implication for the flood damage assessment in the Tondano watershed, North Sulawesi, Indonesia. Modeling Earth Systems and Environment, 2(1). https://doi.org/10.1007/s40808-016-0100-3.
67. Yulianto F, Tjahjono B, Anwar S (2014) The applications of Monte Carlo algorithm and energy cone model to produce the probability of block-and-ash flows of the 2010 eruption of Merapi volcano in

Central Java, Indonesia. Arabian Journal of Geosciences, 8(7):4717–4739. https://doi.org/10.1007/s12517-014-1525-5.

68. Zhang X, Chen X, Zhang W, Peng H, Xu G, Zhao Y, Shen Z (2022) Impact of Land Use Changes on the Surface Runoff and Nutrient Load in the Three Gorges Reservoir Area, China. In Sustainability. (Vol. 14, Issue 4). https://doi.org/10.3390/su14042023.
69. Zhu J (2010) GIS based urban flood inundation modeling. Second WRI Glob Congr Intell Syst 2:140–143.
70. Zoungrana B, Conrad C, Amekudzi L, Thiel M, Da E (2014) Land Use/Cover Response to Rainfall Variability: A Comparing Analysis between NDVI and EVI in the Southwest of Burkina Faso. Climate, 3, 63–77. https://doi.org/10.3390/cli3010063.

Figures

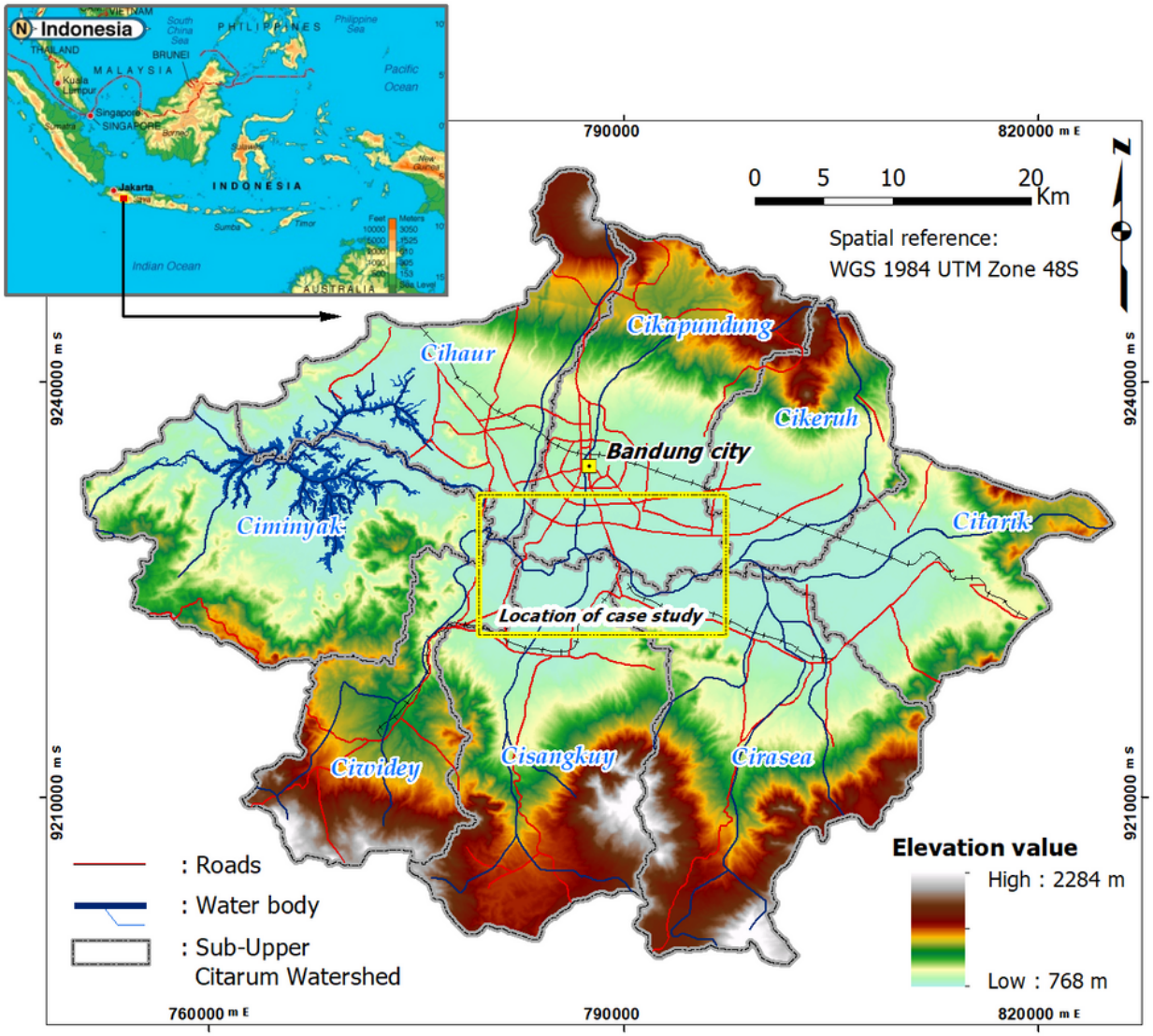

Figure 1

The study area is located in the upstream Citarum, West Java, Indonesia

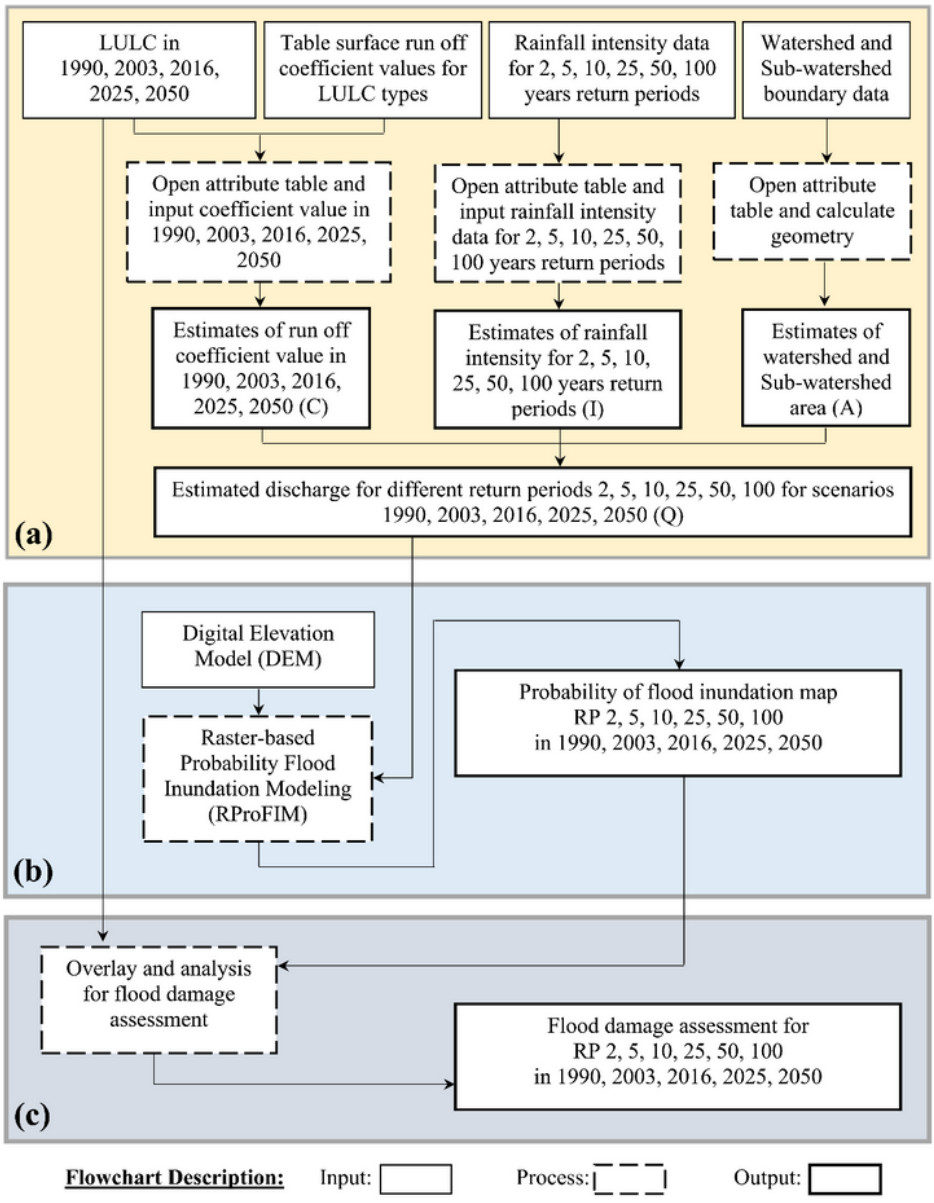

Figure 2

The flow chart used in this study

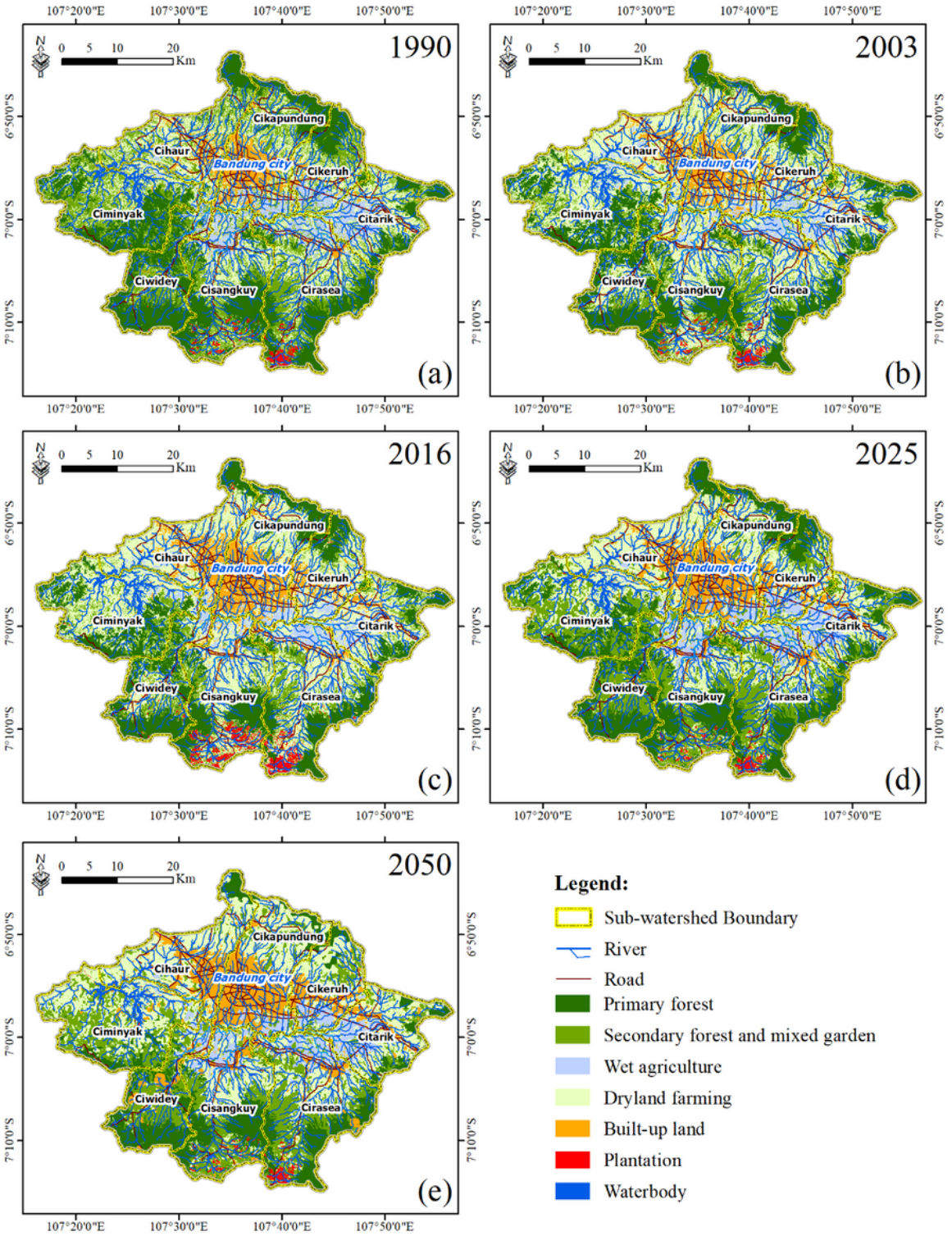

Figure 3

The LULC data is a product of the results of analysis and digital classification of remote sensing data. The LULC data (a) in 1990, (b) in 2003, (c) in 2016 and LULC predictions (d) in 2025 and (e) in 2050 (Source and modified from Yulianto et al., 2019; Yulianto at al., 2020; Yulianto et al. 2022).

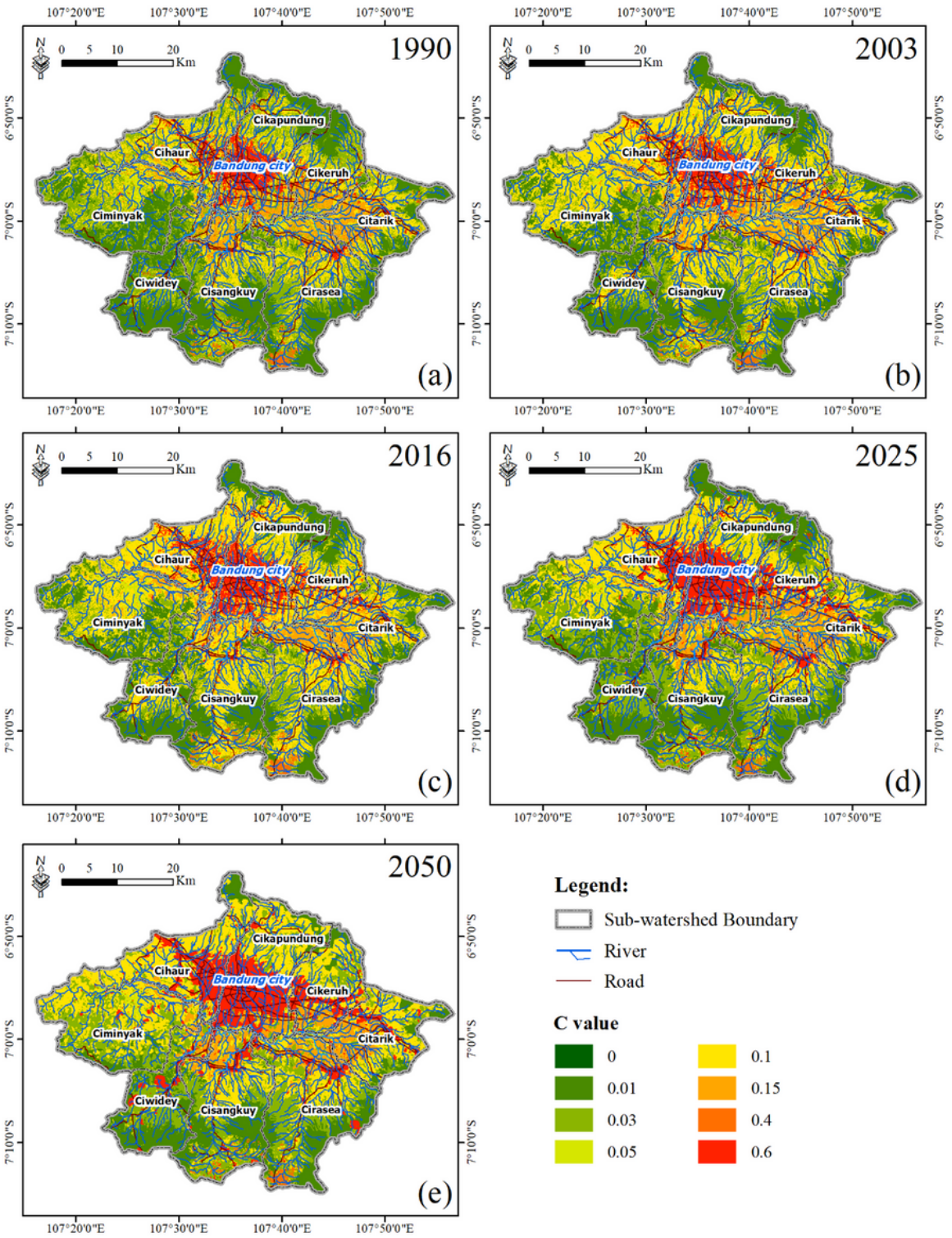

Figure 4

The estimates of run off coefficient value for each LULC. Spatially, run off coefficient value LULC (a) in 1990, (b) in 2003, (c) in 2016 and based on predictions LULC (d) in 2025 and (e) in 2050 (Source and modified from Yulianto et al., 2019; Yulianto at al., 2020; Yulianto et al. 2022).

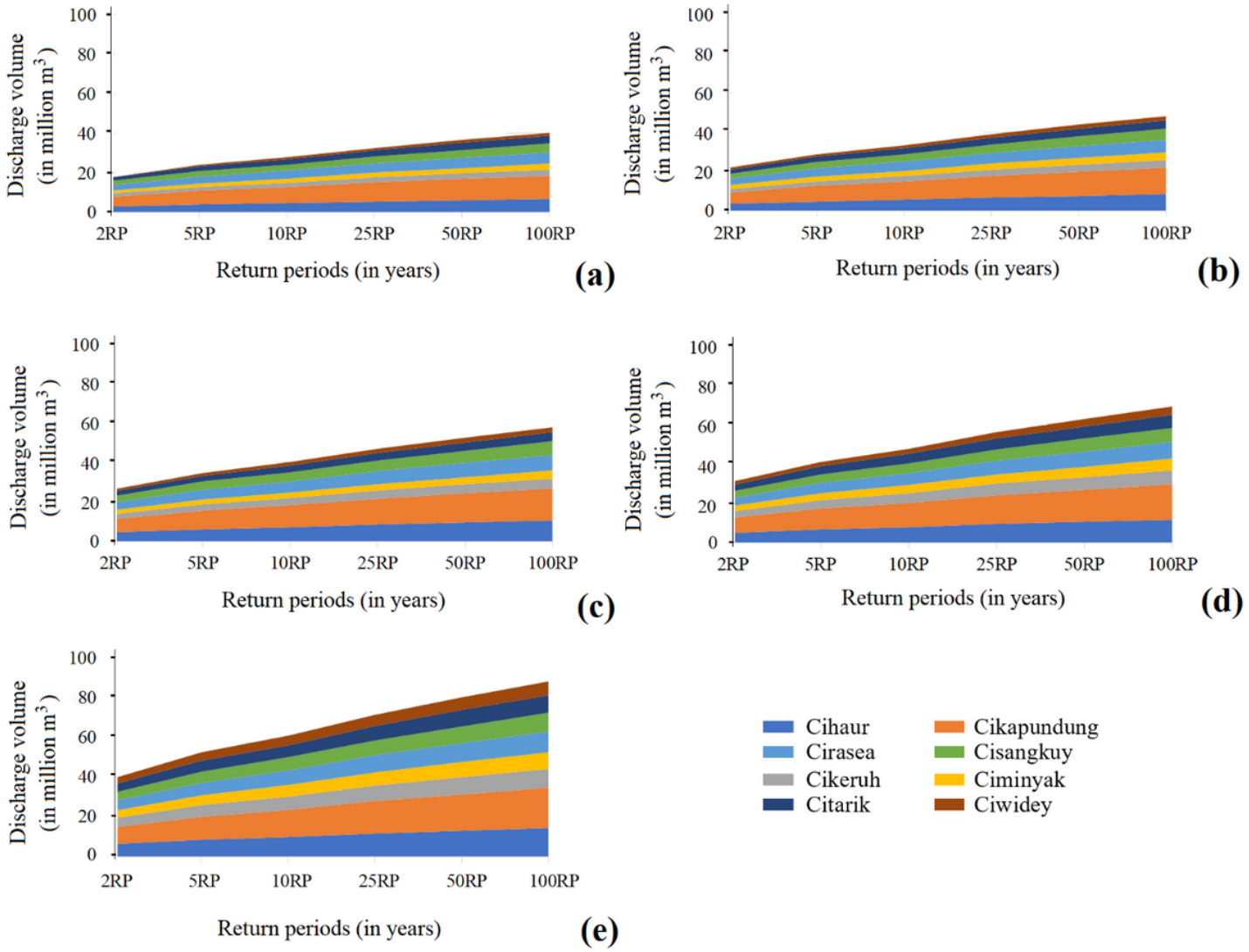

Figure 5

Comparison of the effect of changing LULC on discharge at various return periods in the sub-watershed in study area. (a) scenario LULC in 1990, (b) scenario LULC in 2003, (c) scenario LULC in 2016, (d) scenario LULC in 2025, (e) scenario LULC in 2050.

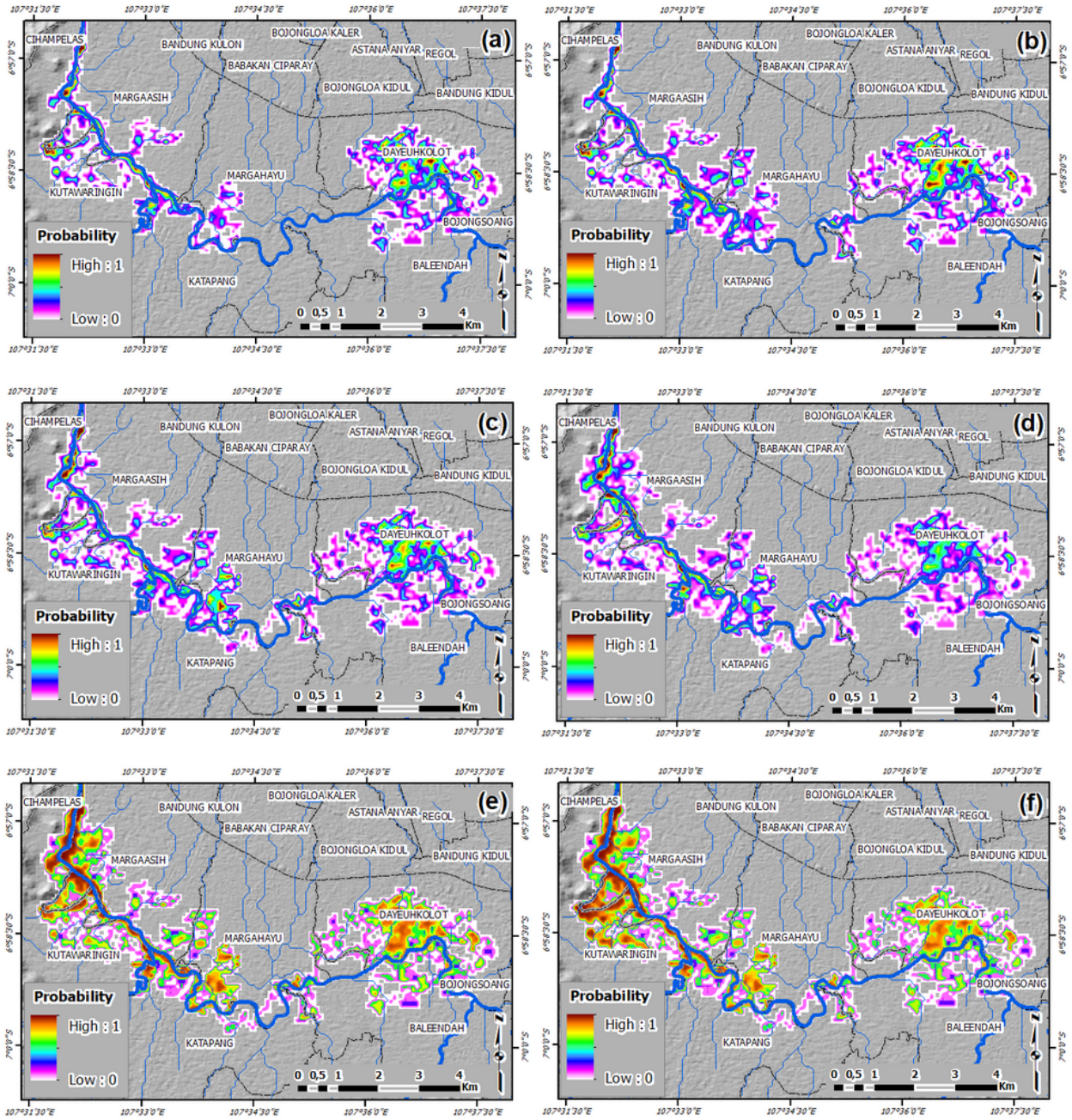

Figure 6

The results of RProFIM model based on the scenario LULC in 1990 and return periods in the study area. (a) scenario return period in 2 year, (b) scenario return period in 5 year, (c) scenario return period in 10 year, (d) scenario return period in 25 year, (e) scenario return period in 50 year, (f) scenario return period in 100 years.

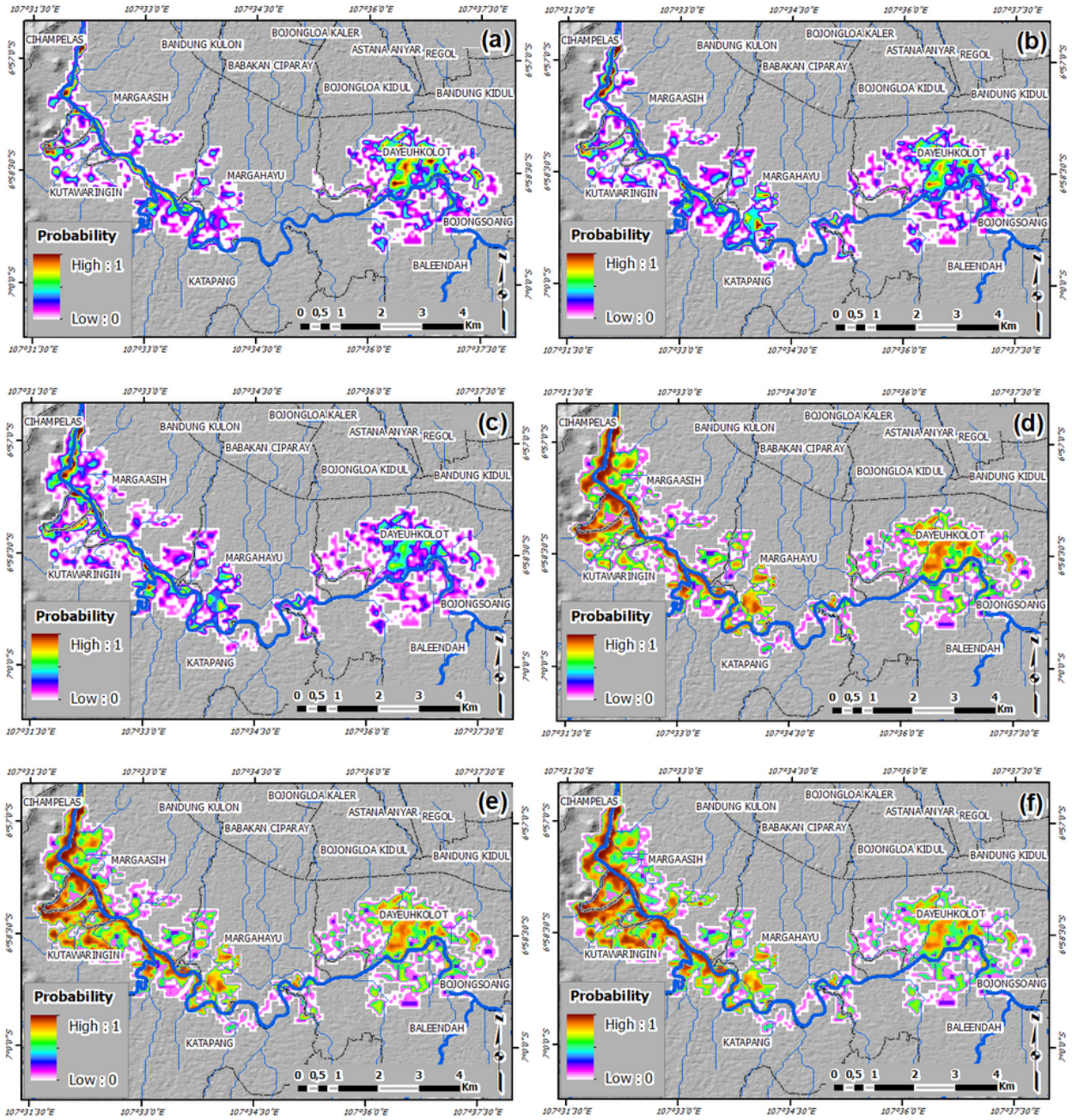

Figure 7

The results of RProFIM model based on the scenario LULC in 2003 and return periods in the study area. (a) scenario return period in 2 year, (b) scenario return period in 5 year, (c) scenario return period in 10 year, (d) scenario return period in 25 year, (e) scenario return period in 50 year, (f) scenario return period in 100 years.

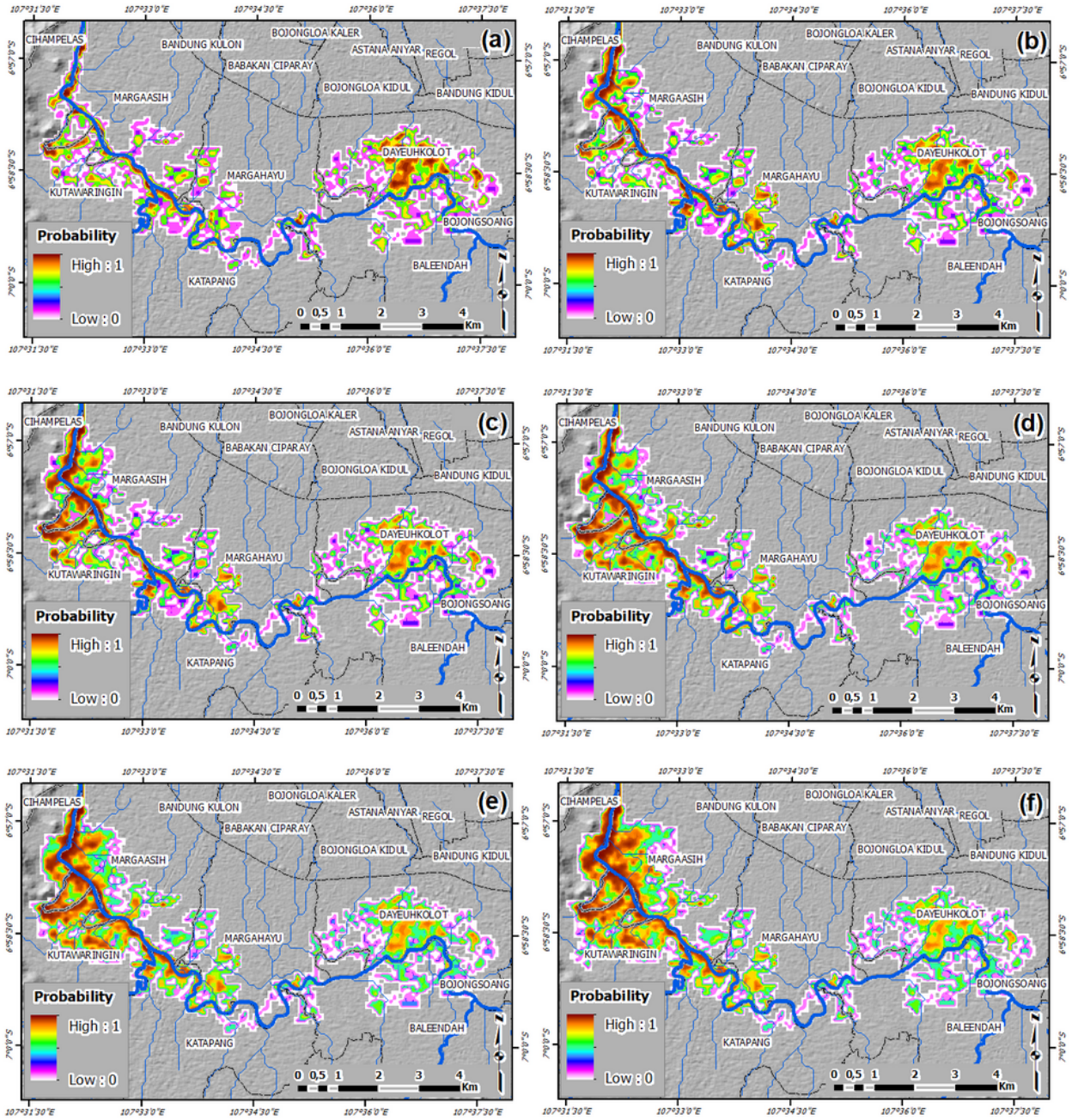

Figure 8

The results of RProFIM model based on the scenario LULC in 2016 and return periods in the study area. (a) scenario return period in 2 year, (b) scenario return period in 5 year, (c) scenario return period in 10 year, (d) scenario return period in 25 year, (e) scenario return period in 50 year, (f) scenario return period in 100 years.

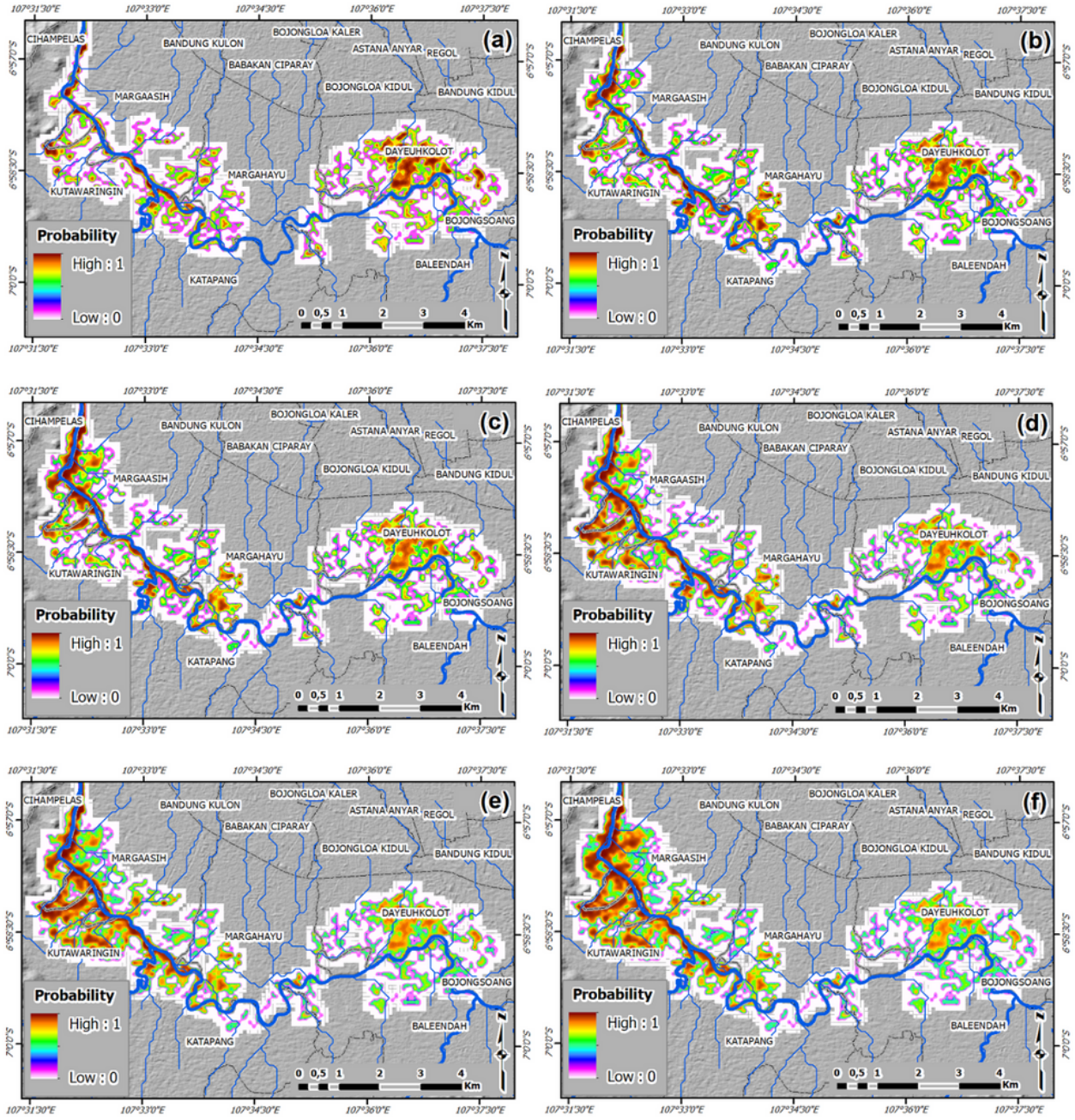

Figure 9

The results of RProFIM model based on the scenario LULC in 2025 and return periods in the study area. (a) scenario return period in 2 year, (b) scenario return period in 5 year, (c) scenario return period in 10 year, (d) scenario return period in 25 year, (e) scenario return period in 50 year, (f) scenario return period in 100 years.

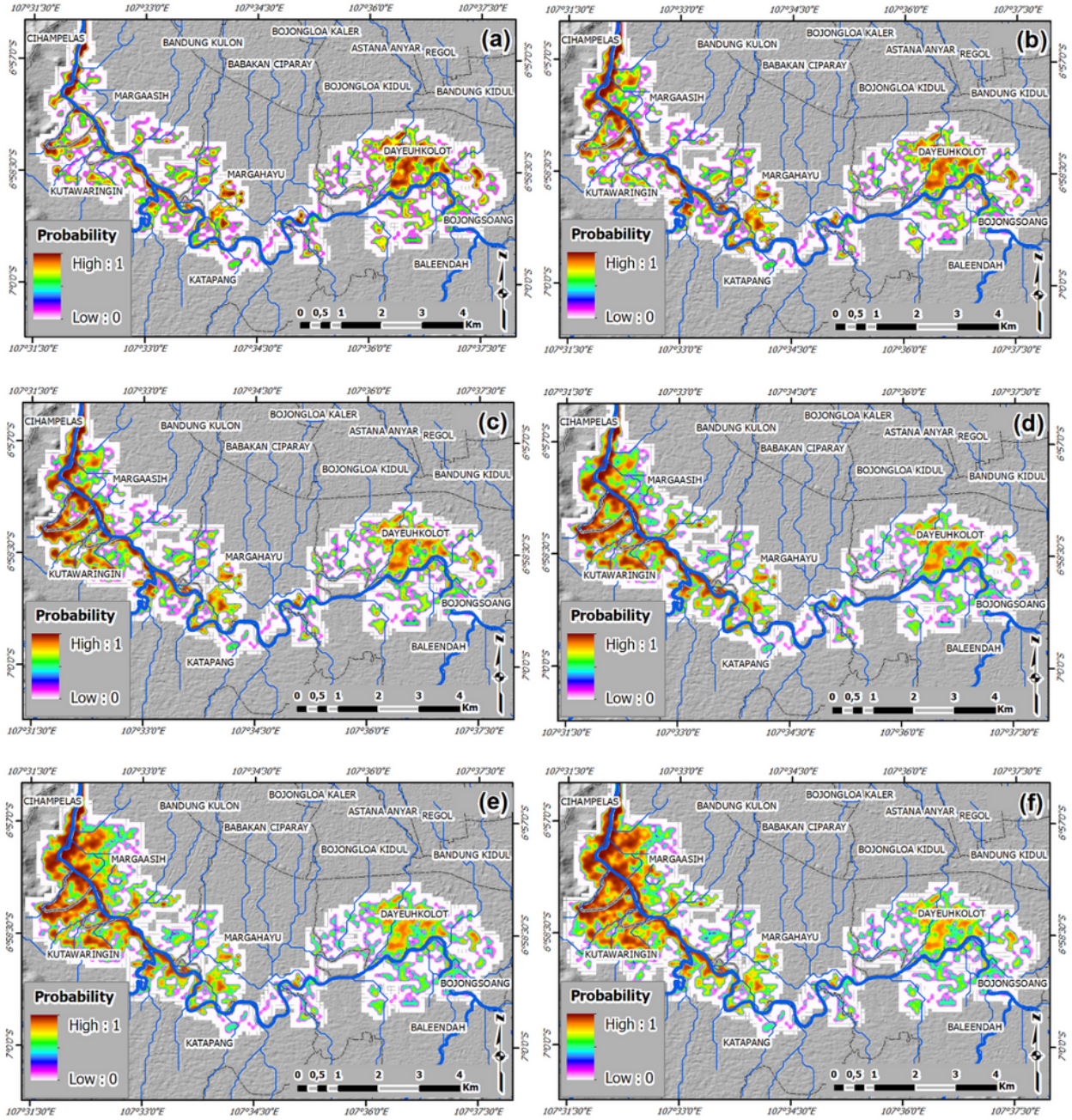

Figure 10

The results of RProFIM model based on the scenario LULC in 2050 and return periods in the study area. (a) scenario return period in 2 year, (b) scenario return period in 5 year, (c) scenario return period in 10 year, (d) scenario return period in 25 year, (e) scenario return period in 50 year, (f) scenario return period in 100 years.

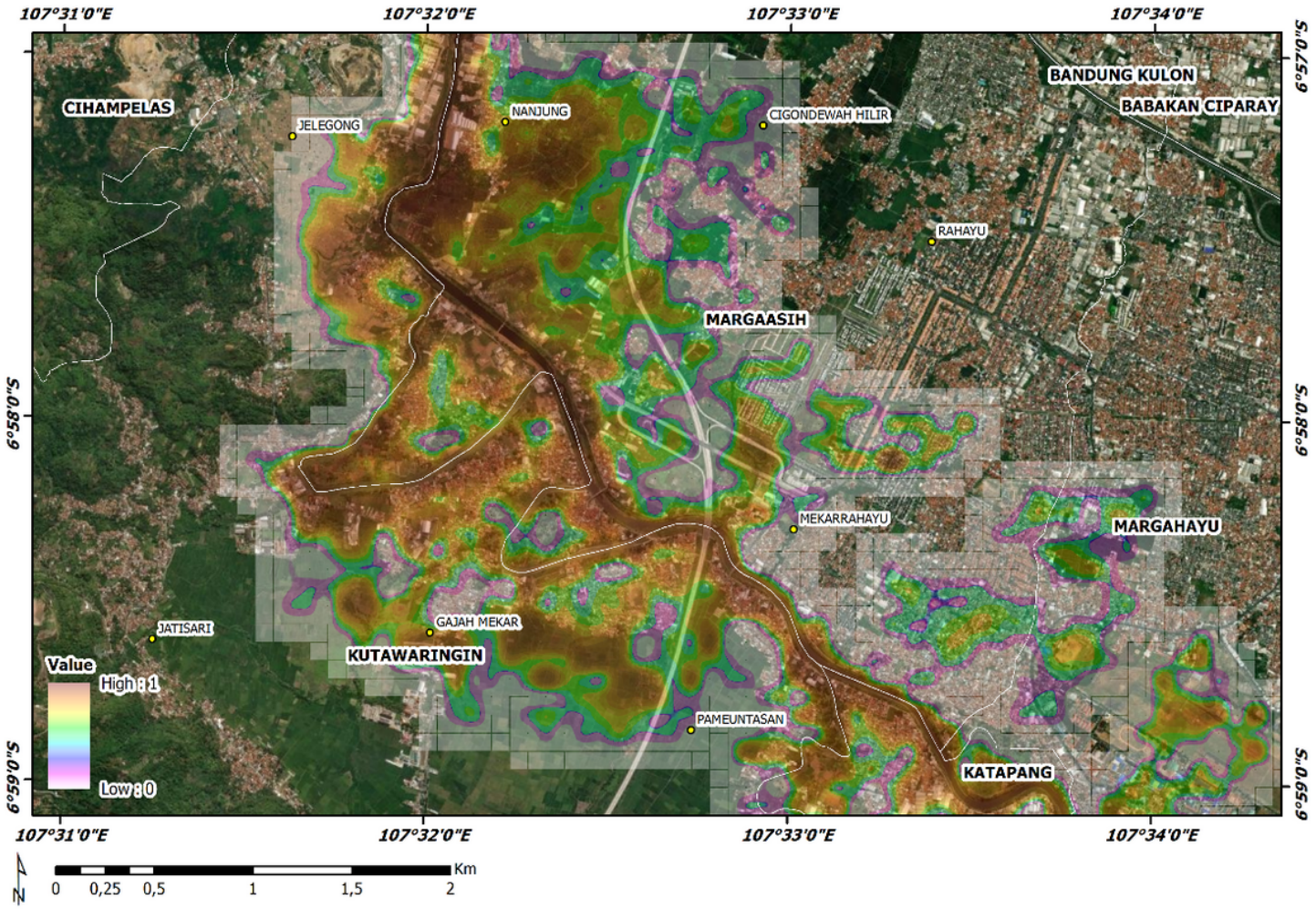

Figure 11

The visual magnification of flood inundation model based on the scenario LULC in 2050 and return period for 100 year. Example in the Margaasih and Kutawaringin districts.

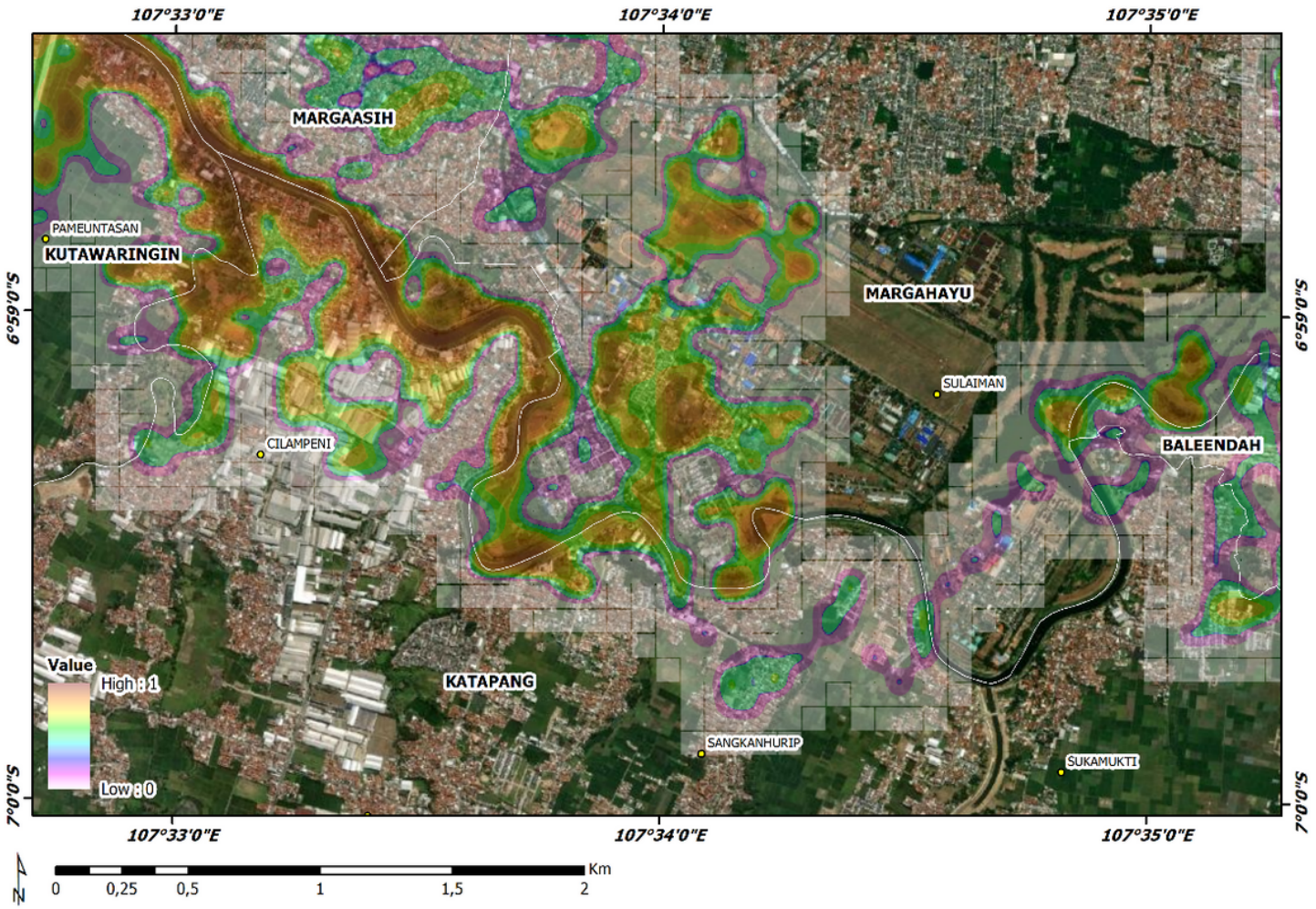

Figure 12

The visual magnification of flood inundation model based on the scenario LULC in 2050 and return period for 100 year. Example in the Margahayu and Katapang districts.

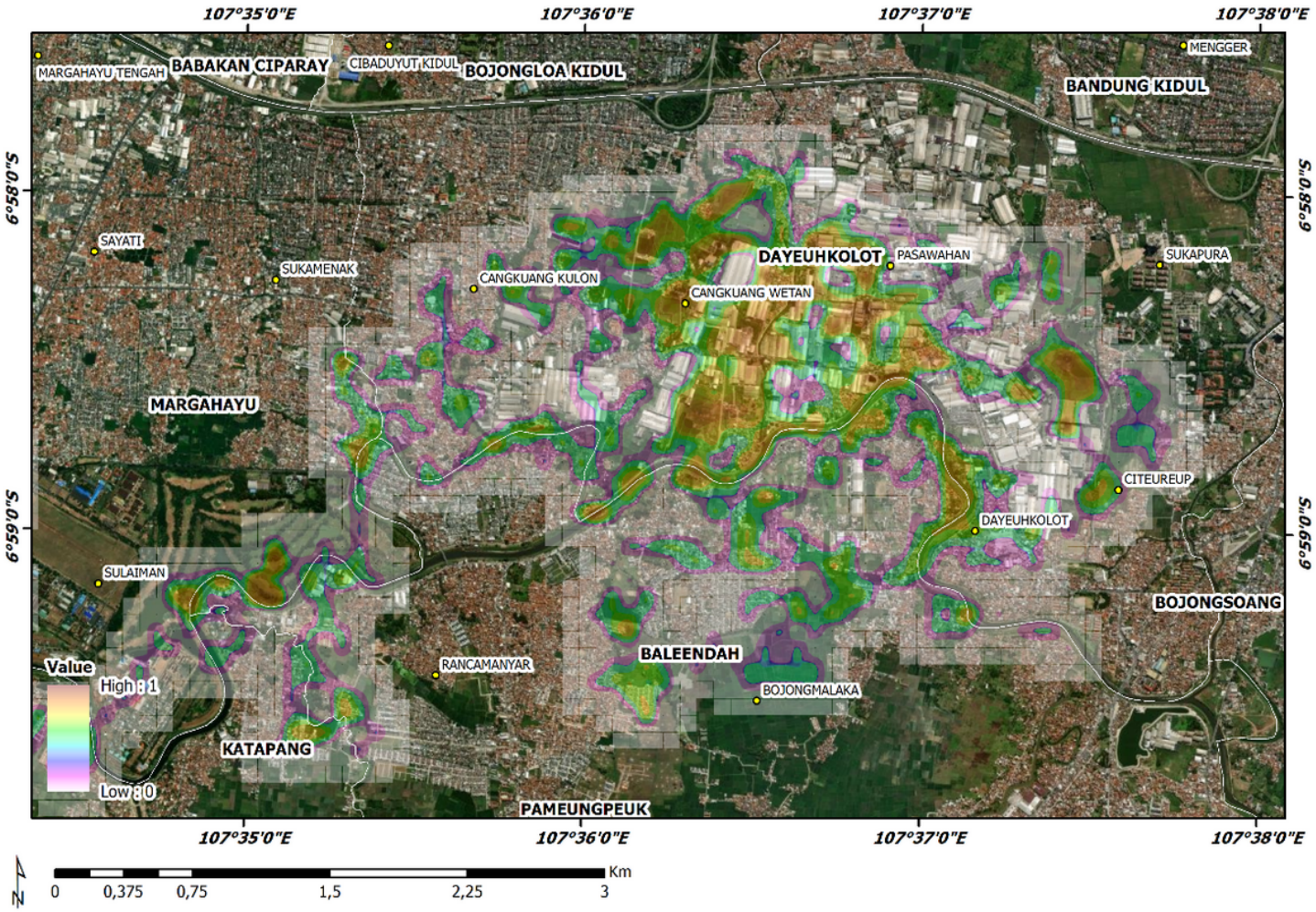

Figure 13

The visual magnification of flood inundation model based on the scenario LULC in 2050 and return period for 100 year. Example in the Dayeuhkolot and Baleendah districts.

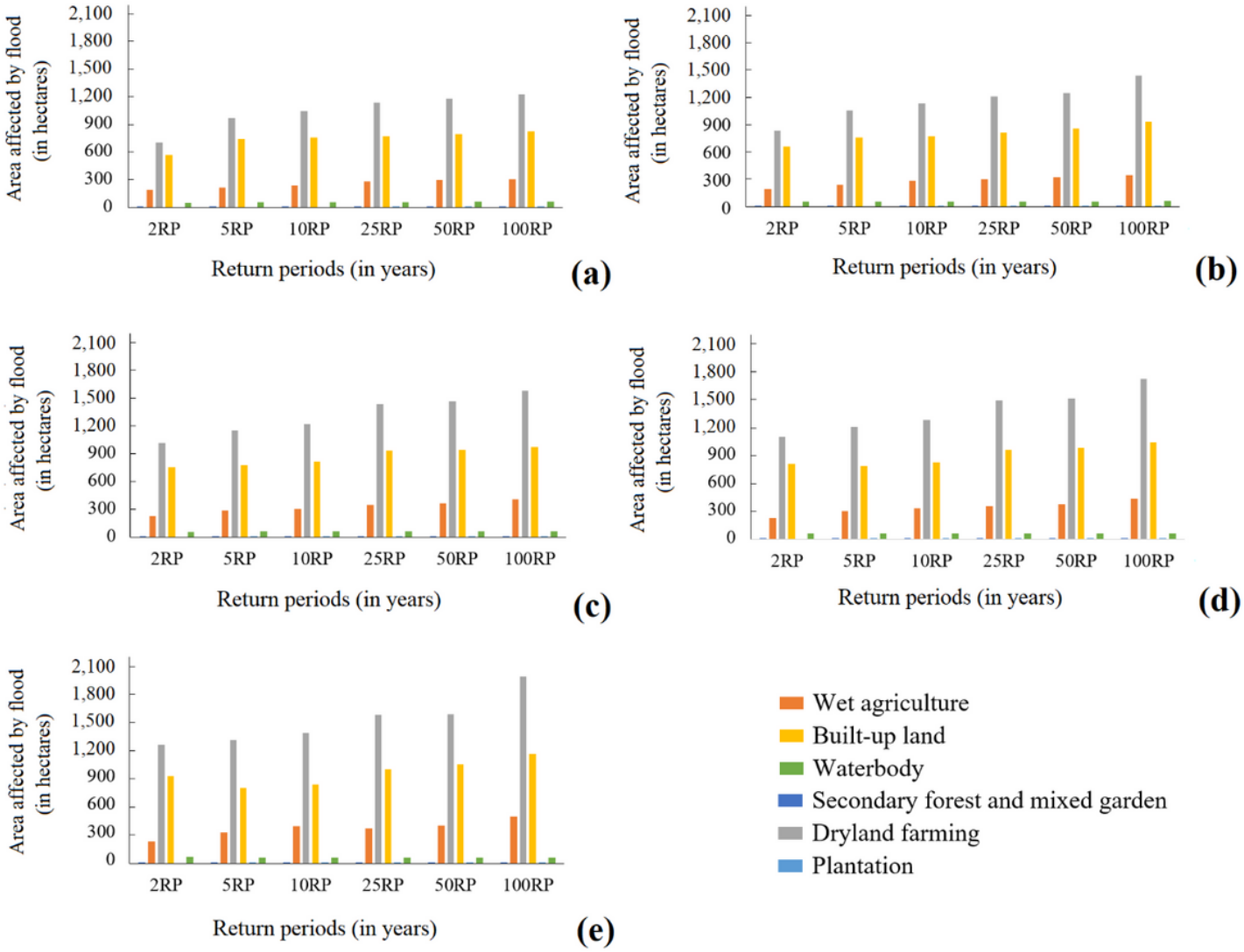

Figure 14

The results of area affected by flood based on overlay of flood inundation map with LULC in various return periods. (a) scenario LULC in 1990, (b) scenario LULC in 2003, (c) scenario LULC in 2016, (d) scenario LULC in 2025, (e) scenario LULC in 2050.

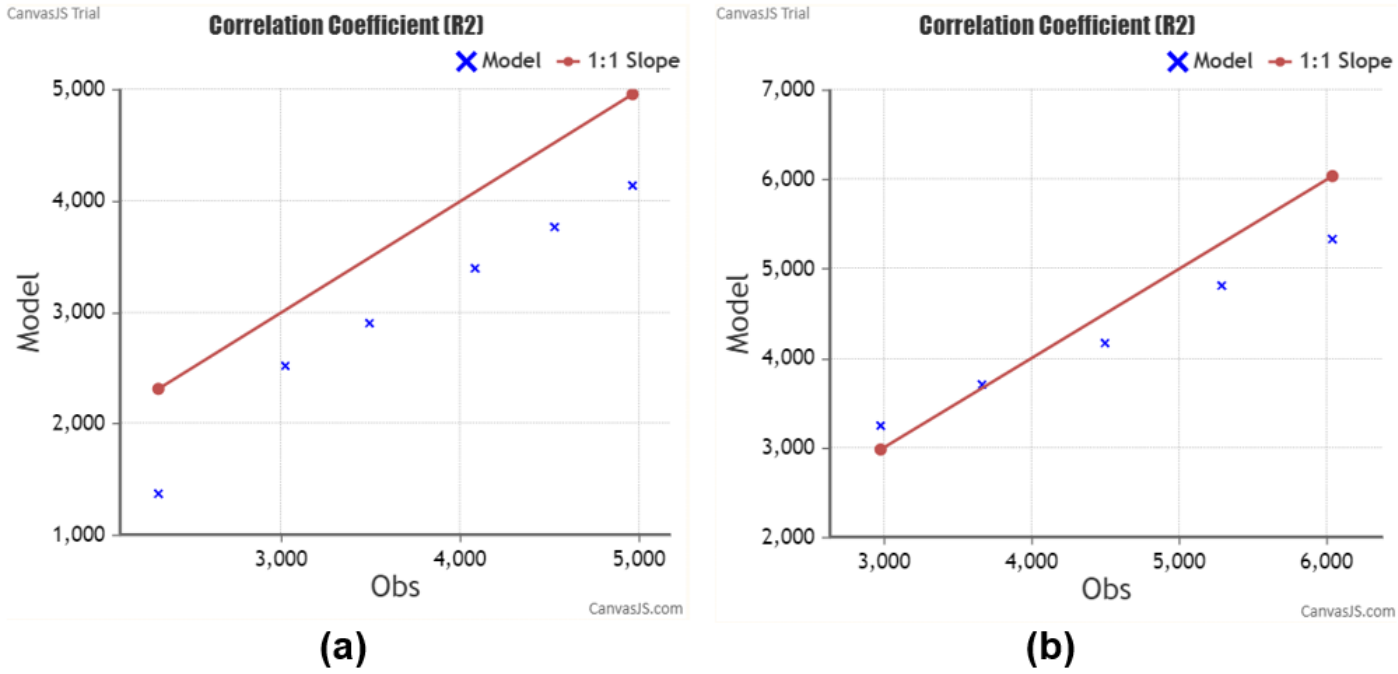

Figure 15

Comparison of the results of the estimated runoff volume in the 2-100 year return period. (a) using the rational method (model) with the SCS-CN (Obs) method from the research by Sentosa et al. (2021) in Cikeruh sub-watershed. (b) using the rational method (model) with the distribusi probabilitas log normal (Obs) from the research by Nuryono et al. (2015) in Cisangkuy sub-watershed.

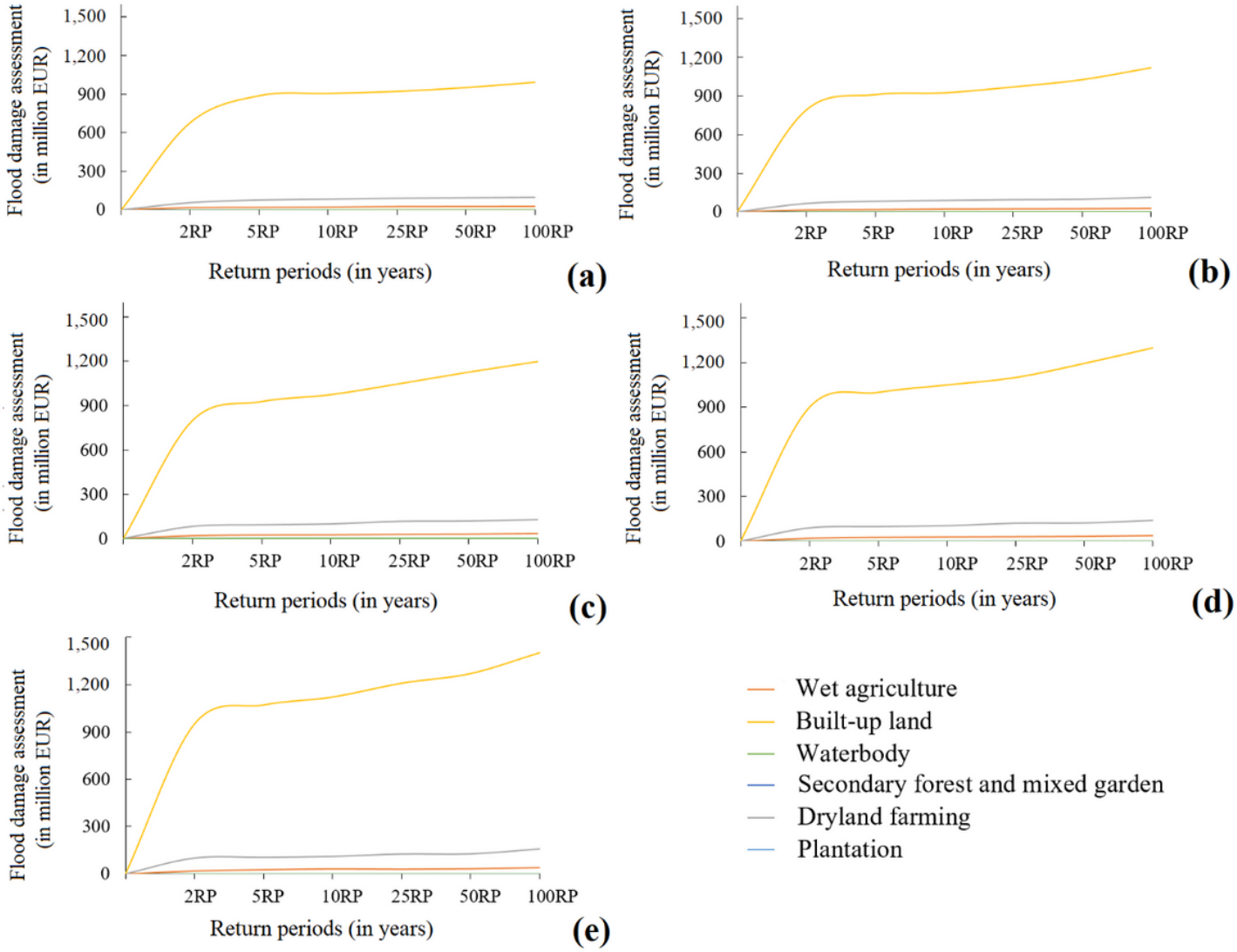

Figure 16

The results of flood damage assessment based on overlay of flood inundation map with LULC in various return periods, which is based on the calculation of market value. (a) scenario LULC in 1990, (b) scenario LULC in 2003, (c) scenario LULC in 2016, (d) scenario LULC in 2025, (e) scenario LULC in 2050.

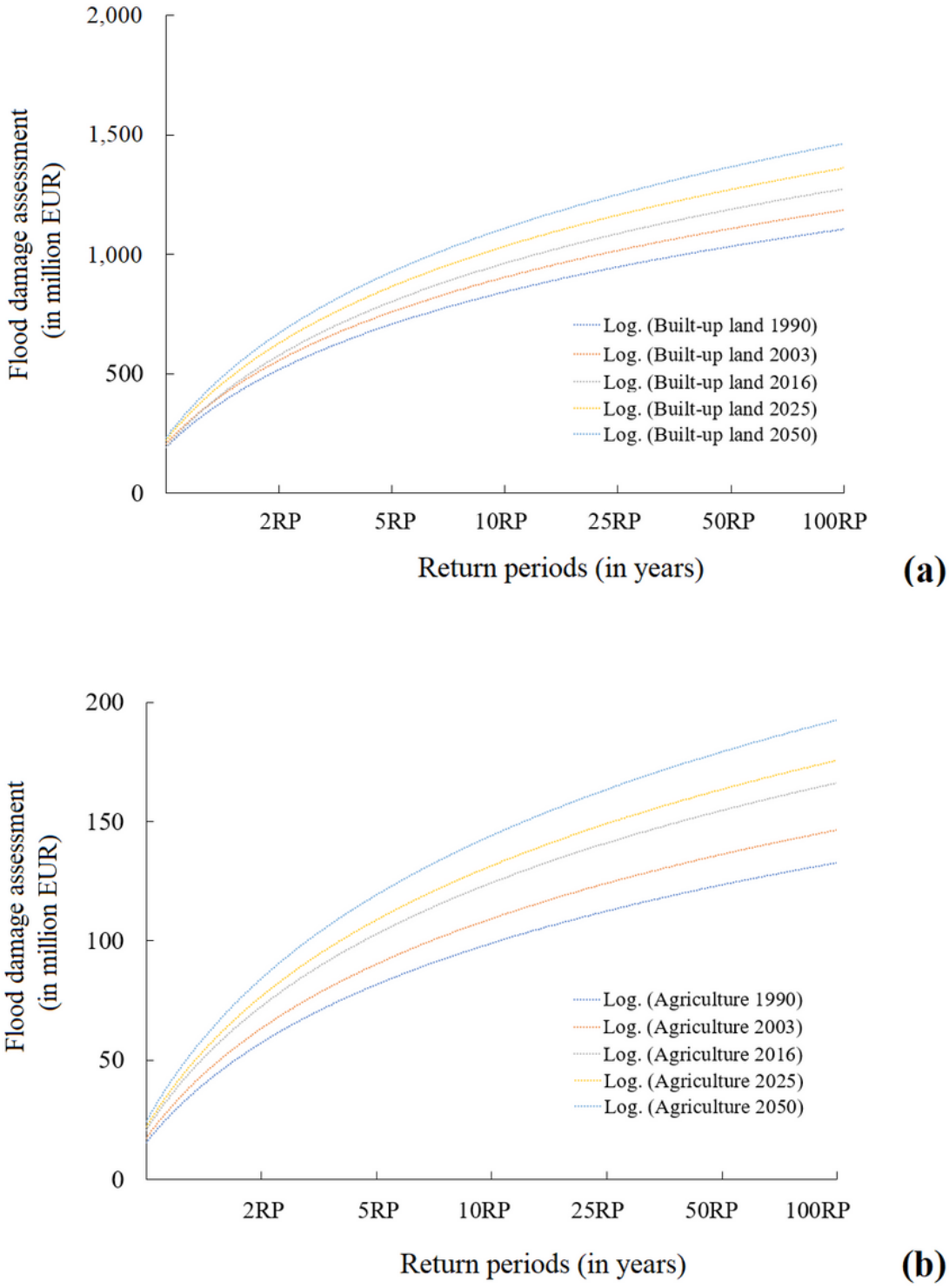

Figure 17

Flood damage assessment model. (a) Flood damage assessment model for built-up land in LULC scenarios ranging 1990 – 2050. (b) Flood damage assessment model for agriculture in LULC scenarios ranging 1990 – 2050.

Supplementary Files

This is a list of supplementary files associated with this preprint. Click to download.

- 00ArticleHighlights.docx